Developmental neurotoxicity of diesel exhaust in a *Gclm* heterozygous mouse model

Ashley Roof Phillips

A thesis

submitted in partial fulfillment of the

requirements for the degree of

Master of Science

University of Washington

2022

Committee:

Toby B. Cole

Lucio G. Costa

Judit Marsillach

Program Authorized to Offer Degree:

Department of Environmental and Occupational Health Sciences

University of Washington

Abstract

Developmental neurotoxicity of diesel exhaust in a *Gclm* heterozygous mouse model

Ashley Roof Phillips

Chair of the Supervisory Committee:

Toby B. Cole

Department of Environmental and Occupational Health Sciences

The 2018 Environmental Performance Index (EPI) named air pollution as the number one environmental threat to public health. Traffic-related air pollution (TRAP) is a sizable contributor to global air pollution, and diesel exhaust (DE) is a major source of TRAP (Yale Center for Environmental Law & Policy, 2018). Though the connection between air pollution and respiratory or cardiovascular diseases is widely known, more recent studies have begun to establish a connection between air pollution and diseases of the central nervous system (CNS). Epidemiological and animal studies have revealed both biochemical and behavioral variations in children or young animals exposed to elevated levels of air pollution, including increased risk of the development of autism spectrum disorder (ASD) (Flores-Pajot *et al.,* 2016). These studies also suggest, much like with cardiovascular impacts, that oxidative stress and neuroinflammation play a large role in the CNS effects. Children diagnosed with ASD show morphological

differences in the brain, high oxidative stress, and neuroinflammation as well as systemic inflammation. Growing evidence supports the notion that ASD is a result of interactions between genetic and environmental factors (Costa *et al.,* 2022, chapter 42). This project measured the gene-environment interaction between the gene encoding *glutamate-cysteine ligase modifier subunit* (*Gclm*), the modulatory subunit of the rate limiting enzyme in glutathione (GSH) synthesis, and neurodevelopmental effects of TRAP exposure. GSH has a key function in combatting oxidative stress and children diagnosed with ASD have shown a 37% increase in GCLM protein and a 38% decrease in glutamate-cysteine ligase (GCL) activity. To study this gene-environment interaction for effects on the neurodevelopmental toxicity of DE, we used a *Gclm* heterozygous ($Gclm^{+/-}$) mouse model, which exhibits decreased GSH-synthesizing activity when challenged with oxidative stress, due to the presence of only one functional *Gclm* allele, hypothesizing that $Gclm^{+/-}$ mice would see exacerbated effects from exposure to diesel exhaust (DE). C57Bl/6 wild-type (WT) dams bred with $Gclm^{+/-}$ sires were exposed to DE or filtered air (FA) throughout gestation, and litters containing the $Gclm^{+/-}$ and $Gclm^{+/+}$ offspring continued to be exposed from post-natal day (PND) 0 to 21. Behavioral endpoints, measured in the offspring at 12 and 24 weeks old, showed deficits in repetitive behaviors and social novelty with DE exposure, but surprisingly these effects were not increased in the $Gclm^{+/-}$ mice. Biochemical endpoints were measured in the brain at 29 weeks old. Lipid peroxidation was higher in the brains of DE-exposed mice, and this effect was exacerbated in $Gclm^{+/-}$ males, but not $Gclm^{+/-}$ females. Finally, a clear effect of DE exposure was seen on neuroinflammation and microglial activation. These effects were not significantly exacerbated in the $Gclm^{+/-}$ mouse model, contrary to what was expected. Thus, the *Gclm* genotype of the offspring, and presumably their altered

ability to induce GSH, was not sufficient to modulate the neurodevelopmental effects of DE exposure.

TABLE OF CONTENTS

Page

LIST OF FIGURES

LIST OF TABLES

ACKNOWLEDGEMENTS

I would like to express my deepest appreciation to my advising committee; Drs. Toby B. Cole, Lucio G. Costa, and Judit Marsillach for their invaluable experience, feedback, and especially for their patience and trust. I am also deeply indebted to the other members of the Costa Lab—Dr. Jacqueline M. Garrick and Khoi Dao, without whom this endeavor would not have been possible. Their support and knowledge, both as colleagues and friends, helped me grow as a researcher and shaped this work. I am grateful to the rest of the DEOHS and the School of Public Health, for their warmth and assistance throughout my time as a student. I received so much support and advice from other students, faculty, even staff and am so incredibly fortunate.

I'd like to recognize Dr. Analena Hope Hassberg, for helping me realize the importance of emphasizing social inequities in all disciplines. She inspired me to pursue graduate work in the field of Public Health, enabling me to study health inequity and environmental risks.

Thank you to my family and friends who have supported me through many ups and downs and who continue to support me now, during the highest of highs. With special thanks to my husband Justin and daughter Edie, for their unrelenting enthusiasm and love for me even in the toughest of times, you both were the anchor I needed. Thank you for the many hours of time you sacrificed in support of my dreams and thank you for your grounding presence.

Finally, this work was made possible through funding from the National Institute of Environmental Health Sciences (NIEHS, R01ES022949, R01ES028273, P30ES07033, P42ES04696), the Eunice Kennedy Shriver National Institute of Child Health and Human Development (U54HD08091), as well as support from the University of Washington and the Department of Environmental and Occupational Health Sciences.

DEDICATION

I dedicate this work to Black, low-income, and other marginalized communities who are disproportionately affected by the adverse health effects of air pollution.

Introduction

1.1 Air pollution and traffic related air pollution

Air pollution (AP) is recognized as the largest global environmental health threat with exposure growing by more than 0.5% a year (UNECE, 2022). AP is composed of many toxicants of concern (*e.g.*, particulate matter [PM], organic and elemental carbon [EC], metals and polycyclic aromatic hydrocarbons [PAHs]), carbon monoxide (CO), ozone (O_3), nitrogen dioxide (NO_2), and sulfur dioxide (SO_2) (Suades-González *et al.,* 2015). According to the Institute for Health Metrics and Evaluation's (IHME) Global Burden of Disease Study, 2019 (GBD 2019) ambient particulate matter exposure was the 7th leading risk factor (up from 9th in 2010) for mortality and disability (IHME, GBD, 2019), accounting for close to 7 million deaths annually (Figure 1.1). Overall AP ranked 4th falling behind only hypertension, smoking, and nutritional factors (Murray

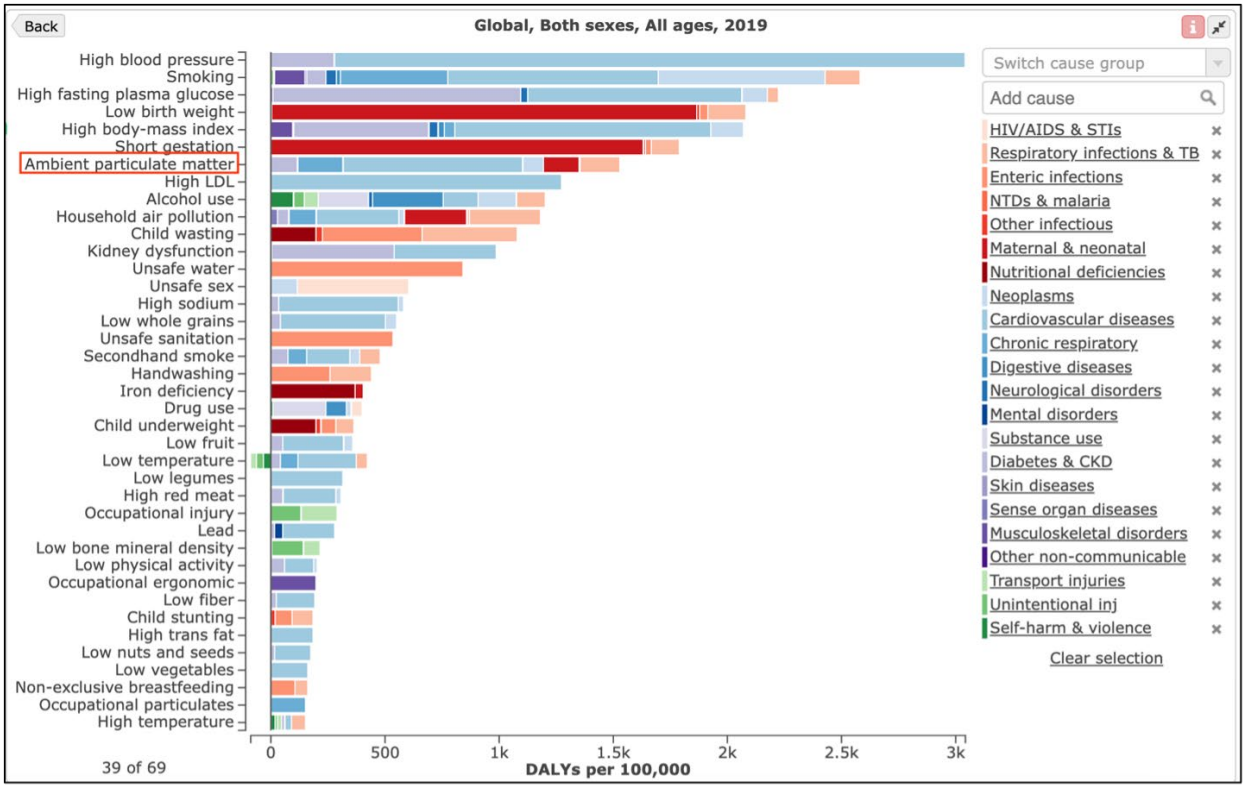

Figure 1.1 Global burden of disease by risk factor, 2019. *Total disease burden, measured in Disability-Adjusted Life Years (DALYs) by sub-category of risk factor, with colors representing cause.*
Source: IHME, Global Burden of Disease, https://vizhub.healthdata.org/gbd-compare/

et al., 2020). Though mortality rates often drive regulation regarding emissions, a growing body of evidence over the past decade has prompted research concerning non-fatal health risks, like those concerning the central nervous system (CNS) (Costa *et al.,* 2022, chapter 42). Several epidemiological studies have demonstrated an association between exposure to AP and increased risk of neurodevelopmental disorders including autism spectrum disorder (ASD), attention deficit hyperactive disorder (ADHD) as well as neuropathological changes such as decreased white matter and altered brain structure (Cory-Slechta *et al.,* 2019).

Particulates are especially pertinent to effects in the CNS (Bandyopadhyay*,* 2016). PM is categorized by its aerodynamic diameter (coarse-ultrafine) with PM_{10} being < 10 μm, $PM_{2.5}$ including particles < 2.5 μm, and ultrafine particles (UFP) comprising all particles under 100 nm. Many organic and inorganic contaminants can be adsorbed by UFPs contributing to the toxicity of UFPM: these contaminants include polychlorinated biphenyls (PCBs), PAHs, and small metals (Cory-Slechta *et al*., 2019). Fine particles are associated with more serious health implications due to the ability of these particles to enter circulation in the bloodstream and distribute to other organs, including the heart and brain (Morris-Schaffer *et al.,* 2019a). These UFPs are also able to deposit in the nasal cavity and translocate along the olfactory nerve directly to the olfactory bulb (Oberdörster *et al.,* 2004). UFPM is mainly combustion-derived and therefore of considerable interest when vehicular emissions have been shown to contribute 65% of particles in this size range (Pey *et al.,* 2009).

For much of the world, traffic (along with industrial emissions) is a major source of air pollution. This mixture of pollutants is known as traffic-related air pollution (TRAP). For many pollutants,

TRAP contributes 25–40% of the ambient levels (Greenbaum, 2013, chapter 5). This number can vary depending on proximity to urban centers, urban design, and proximity to freeways (Hankey *et al.,* 2012). TRAP is the main source of UFPM in urban areas and with urbanization consistently escalating, worldwide population exposure is sure to climb as well (Kumar *et al.,* 2014). While the 2021 World Health Organization Global Air Quality Guidelines (WHO AQG) advocate for annual concentrations of $PM_{2.5}$ under 5.0 $\mu g/m^3$ and the United States Environmental Protection Agency (US EPA) National Ambient Air Quality Standard is 12.0 $\mu g/m^3$, unregulated pollutants like UFPs are a growing problem. The follow-up to the landmark Harvard Six Cities study confirmed that an increase of 10.0 $\mu g/m^3$ of $PM_{2.5}$ was associated with an increased mortality risk of 14%. This association was linear as low as 8.0 $\mu g/m^3$ and this trend is presumed to be similar for UFPM (Lepeule *et al.,* 2012, Morris-Schaffer *et al.,* 2019b). Despite worldwide regulations, ambient AP numbers continue to rise due to significant drivers that include intense city growth, escalating energy needs, and increased use of gas fueled transportation, leaving more than 90% of the world living in regions that do not meet the WHO's healthy air standards (Myers & Frumkin, 2020).

1.1.1 Diesel exhaust exposure model

Diesel exhaust (DE) is a major component of global air pollution in urban areas and is frequently used in exposure experiments to investigate responses to TRAP (Long, 2022). DE is comprised of more than 40 pollutants and is a major contributor to ambient PM levels, therefore it is commonly considered the most important component of TRAP (USEPA, 2002, Costa *et al.,* 2017). Previously in our lab, acute exposure of environmentally-relevant concentrations (250-300 $\mu g/m^3$) of DE was shown to increase microglial activation (increased Iba1) and lipid

peroxidation in several brain regions of 3-month-old C57BL/6 mice. These exposures also led to increased levels of pro-inflammatory cytokines [interleukin 6 (IL-6), interleukin-1-alpha (IL-1α), interleukin-1-beta (IL-1β), interleukin 3 (IL-3), and tumor necrosis factor alpha (TNFα)] in these same brain regions, with significant effects shown in the olfactory bulb and hippocampus. Another study also examined the role of gene-environment interactions in DE-induced neurotoxicity through utilization of a *Gclm* knockout mouse model (*Gclm*$^{-/-}$), which exhibits impaired glutathione (GSH) synthesis in mice homozygous (*Gclm*$^{-/-}$) or heterozygous (*Gclm*$^{+/-}$) for the deletion. Results showed that the *Gclm*$^{+/-}$ mice had increased levels of proinflammatory cytokines, IL-3 and IL-6, in both the olfactory bulb and hippocampus when compared to WT and *Gclm*$^{-/-}$ mice (Cole *et al.,* 2016). A preliminary investigation of the *Gclm* polymorphism involving adult male mice exposed acutely to DE had shown increases in oxidative stress and neuroinflammation that were exacerbated in both *Gclm*$^{-/-}$ and *Gclm*$^{+/-}$ mice (Costa *et al.,* 2014a). Subsequent studies explored developmental exposure to DE (250-300 μg/m^3) from embryonic day (E) 0 to post-natal day 21 (PND21). These results yielded deficits in three hallmark ASD behaviors: social interactions, repetitive behaviors, and altered communications; as well as increased IL-6, signal transducer and activator of transcription 3 (STAT3), and DNA methyltransferase 1 (DNMT1), shown to be vital participants in ASD etiology via down regulation of reelin (RELN) and consequent cortical laminar disorganization (Chang *et al.,* 2018, 2019).

Roqué *et al.* found that diesel exhaust particles (DEP) in a concentration of 25-100 μg/2 m^2 were toxic to 7-day-old C57Bl/6J mice cerebellar granule neurons (CGN) in a co-culture with microglia, and that microglia were necessary for the neurotoxicity. DEP activated the microglia

and increased expression of pro-inflammatory mediators such as IL-6 (Roqué *et al.,* 2016). The composition of DE varies due to numerous parameters, from engine and fuel type to built environment. Because of this variation environmental DE is complicated to simulate, leaving controlled exposures as the ideal for studying the mechanisms of health effects (Fox *et al.,* 2015). The model of controlled DE exposure used for the current study (see Fig. 2.1 for schematic) allows us to dilute the NO_2 to separate its effects from DE, both of which have diverse toxicological outcomes (Long *et al.,* 2022). To further test these interactions, the current study exposed the mice identically to the previous studies (Chang *et al.,* 2018, 2019) at the University of Washington's (UW) Northlake Controlled Exposure Facility. C57Bl/6 dams were exposed perinatally to 250-300 $\mu g/m^3$ DE (of FA) from E0 until birth (PND0), with the dam and offspring ($Gclm^{+/+}$, $Gclm^{+/-}$) continuing to be exposed until PND21.

1.2 Health effects of air pollution

In 2010, the Health Effects Institute (HEI) conducted a systematic review on the health effects of TRAP, finding strong associations with cardiovascular and pulmonary outcomes. Though TRAP is a mixture of many toxicants, PM is thought to be the most associated with adverse health outcomes (Nephew *et al.,* 2020). $PM_{2.5}$ and PM_{10} are in the range of respirable particles, while the larger particles are stopped in the nose and upper respiratory tract. $PM_{2.5}$ can enter the CNS through the olfactory epithelium or through the pulmonary systems causing many neurotoxicological effects (Bandyopadhyay, 2016). UFPM has also been discovered in the olfactory bulbs of children exposed to high levels of air pollution, demonstrating the olfactory nerve as a route of particular concern (Calderón-Garcidueñas *et al.,* 2010; Oberdörster *et al.,* 2004). Systemic inflammation and oxidative stress have proven to be primary drivers associated

with the adverse effects of AP on the cardiovascular and pulmonary systems, including ischemic stroke and heart disease (Brook *et al.,* 2010; Maheswaran, 2016). Inflammation and oxidative stress are very closely related in their response to air pollution. Production of free radicals and reactive oxygen species (ROS) is a natural result of mitochondrial respiration, and an oxidoreductive balance is necessary to regulate certain functions. This balance is thrown off by air pollution as both organic and inorganic particles can directly generate ROS, which encourages lipid peroxidation, nucleic acid damage, and protein disruption (Jankowska-Kieltyka *et al.,* 2021). Generation of ROS can also impact macrophages and their inflammatory processes, which involves the release of many inflammatory mediators (Costa *et al.,* 2016). Instigation of the immune system can cause a similar reaction directly in the CNS through activation of microglia and release of chemokines, free radicals, and production of cytotoxic cytokines (Jankowska-Kieltyka *et al.,* 2021).

The association of PM with respiratory and cardiovascular diseases has been substantiated in multiple studies (Bourdrel *et al.,* 2017; Brook *et al.,* 2010; Gill *et al.,* 2011; Mookherjee *et al.,* 2022; Wang *et al.,* 2019; Wu *et al.,* 2019). Mounting studies also indicate TRAP as a risk factor for cognitive impairment and neurodegeneration (Costa *et al.,* 2020; McGuinn *et al.,* 2022; Nephew *et al.,* 2020; Salvi & Salim, 2019; Schraufnagel *et al.,* 2019). DE, the most significant driver of disease in TRAP, has been linked to respiratory issues, cardiovascular dysfunction, developmental neurotoxicity, and neurodegeneration, and is also considered “carcinogenic to humans” by the International Agency for Research on Cancer (IARC) (Weitekamp *et al.,* 2020). In addition to these findings, there have been substantial effects found in the reproductive system, with consistent changes in both testosterone and progesterone levels reported in males

and females, respectively (Li C *et al.,* 2019). Outdoor air pollution was responsible for approximately 4.2 million deaths in 2015; without uncompromising interventions, these numbers are expected to grow to 6.6 million yearly by 2050 (Myers and Frumkin, 2020).

1.2.1 Neurotoxicity of air pollution

In the decade since the HEI review was published the body of evidence regarding AP's effects on nearly all other essential body systems has grown considerably, especially regarding the CNS (Block & Calderón-Garcidueñas, 2009, Calderón-Garcidueñas *et al.,* 2016; Cole *et al.,* 2020; Chang *et al.,* 2019; Costa *et al.,* 2014a, 2014b, 2017). These effects are thought to be due to PM's ability to cross the body's barriers and access peripheral circulation, though as described earlier direct olfactory entry is also involved (Block & Calderón-Garcidueñas, 2009; Jankowska-Kieltyka *et al.,* 2021). These CNS effects could also be occurring indirectly as $PM_{2.5}$ has recognized effects in the cardiovascular system, where disease has historically appeared to promote cognitive deficits and dementia (Power *et al.,* 2016).

Neurodegenerative diseases have grown in prevalence since 1990; Alzheimer's Disease (AD) has increased by 145% while Parkinson's Disease (PD) has grown by 117% (Shi *et al.,* 2010). Air pollution has been linked with neurodegenerative disorders as early as 2002, in a study evaluating a feral dog cohort in Mexico City, where healthy human populations exposed to significant pollutants had shown respiratory damage. The dogs were shown to have extensive CNS damage including altered blood brain barrier (BBB), damaged cortical structure, apoptotic glial cells, and neurofibrillary tangles (Calderón-Garcidueñas *et al.,* 2002). With an aging population worldwide, the impact of AP on neurodegeneration has been represented by a

growing body of work in the field (Jankowski-Kieltyka *et al.,* 2021). Experiments carried out in rats exposed to DE showed neuroinflammation and increases in markers associated with both AD and PD (Levesque *et al.,* 2011). A longitudinal study conducted in 2020 found that a diagnosis for AD or PD during a first hospital visit increased linearly with increasing exposure to $PM_{2.5}$ at or below the national standards, suggesting that no safe limit exists for these pollutants (Shi *et al.,* 2020).

Epidemiological evidence shows that AP is implicated in decreased cognitive function at all stages of life, with increased sensitivity in children and the elderly (Chen & Schwartz*,* 2009; Kilian & Kitazawa, 2018; Power *et al.,* 2016; Xu *et al.,* 2016). A prospective study of school-aged children found that children from schools with high levels of TRAP had smaller growth in cognitive development (7.4%) when compared with children from schools with low TRAP levels (11.5%) (Sunyer *et al.,* 2015).

Inflammation has been an area of focus for CNS effects because it is such a strong driver for diseases of the cardiovascular and pulmonary systems. A correlation between inflammation in the CNS and AP has been previously demonstrated *in vivo* in animals and humans, as well as *in vitro* (Cole *et al.,* 2016; Roqué *et al.,* 2016; Costa *et al.,* 2017, 2019). Prenatal exposure to AP has been associated with a systemic inflammatory response, potentially resulting in neuronal injury (Chun *et al.,* 2020).

1.2.2 Developmental neurotoxicity of air pollution

Epidemiological studies have shown an association between exposure to AP and increased risk of ASD, ADHD, slowing of cognitive development, and schizophrenia (Cory-Slechta *et al.,* 2019). Adverse effects on neurodevelopment have also been shown to be associated with TRAP (Jung *et al.,* 2013; Volk *et al.,* 2014, 2013). The development of the nervous system is particularly vulnerable to environmental stressors because of its dependence on critical processes (*i.e.*, proliferation, migration, differentiation, synaptogenesis, myelination, and apoptosis). The neurodevelopmental stage spans the embryonic period through adolescence, making it an extensive phase of growth (Suades-González *et al.,* 2015; Rice & Barone, 2000).

As previously described, TRAP, and DE specifically, is a complex mixture with many toxicants of concern. Previous studies have shown prenatal DE exposure of 1.0 mg/m^3 caused variations in motor activity, motor coordination, and impulse behaviors in mice (Yokota *et al.,* 2013; Suzuki *et al*., 2010). A review from 2018 showed that *in utero* exposure to PAHs, a component of PM, could be correlated with reduced IQ scores in children ages 3-7 (Kilian & Kitazawa, 2018). Another meta-analysis, comparing effects of PM as well as NO_2, showed only an association between NO_2 and psychomotor development (Guxens *et al.,* 2014). Two studies concentrated on black carbon, a significant short-lived component of DE, and showed that an environmental increase in black carbon was inversely correlated to IQ, vocabulary, learning, and memory in children ranging 7-14 years of age (Chiu *et al.,* 2013; Suglia *et al.,* 2008).

Though mechanisms by which this association occurs are not well understood, it is probable that oxidative stress and neuroinflammation play a key role (Costa *et al.,* 2019, chapter 7). Animal

studies focused on inflammatory pathways have shown that DE exposure increased oxidative stress and neuroinflammation, including an increase of primary cytokines—IL-6, IL-1β, interferon-gamma (IFNγ), and tumor necrosis factor alpha (TNFα) (Bai *et al.,* 2019; Cole *et al.,* 2016; Kraft & Harry, 2011; Nephew *et al.,* 2020). In the Mexico City cohort, where participants live under conditions of extreme air pollution, evidence was found of olfactory bulb inflammation, systemic inflammation, and brain inflammation, as well as cognitive deficits (Calderón-Garcidueñas *et al.,* 2002, 2010, 2016). Because of its ubiquitous nature and varying prevalence, ASD has become a key research area when investigating these neurodevelopmental effects (Zeidan *et al.,* 2022).

1.2.3 Autism spectrum disorder and air pollution

ASD includes a range of disorders with varying symptoms that typically manifest before 3 years of age (Rice *et al.,* 2012). These symptoms include impairments in social interactions, verbal and non-verbal communication, as well as significant motor deficits (Jung *et al.,* 2013). ASD prevalence has increased from 4 per 10,000 (40 years ago) to 30-60 cases per 10,000, which can be linked to improved diagnostic techniques, but environmental and genetic risk factors have also been shown to be associated with this increase (Rutter *et al.,* 2005). In a study conducted in 2014 by Sandin *et al.,* the probably of an ASD diagnosis when a sibling had an ASD diagnosis was 13% compared to 1.2% without a diagnosis.

Though there is a clear genetic component to ASD etiology, the evidence continues to mount for AP as an environmental contributor. The current theory is that distinct environmental factors paired with genetic interactions lead to ASD. A study that estimated childhood exposure to PM

in each trimester showed that increased maternal exposure to PM led to an increased odds of ASD diagnosis (Raz *et al.,* 2015). Another study showed a two-fold increase in ASD diagnosis associated with residential proximity to freeways during gestation and the first year of life (Volk *et al.,* 2011). In 2013, Roberts *et al.* showed that an increase in exposures to diesel emissions and metals associated with AP was linked with an increase in ASD diagnosis. A systematic review published in 2019 showed that 3rd trimester exposure to AP was a consistent trend among studies linking developmental exposure and ASD (Chun *et al.,* 2020). Myelination starts in the late 2nd trimester and continues through the first year of life, and imaging shows a deficit of myelination in the brains of ASD diagnosed children when compared to typically developing children (Aoki *et al.,* 2013; Zikopoulos & Barbas, 2010). These findings support the need for assessing perinatal air pollution exposure when examining these ASD-related effects.

Though evidence has emerged to the cause of ASD, be it environmental, genetic, or both, the pathophysiology of the disorder is not well established. Dysregulated neuroinflammation is an evolving model to explain the etiology of ASD (Matta *et al.,* 2019). Along with air pollution and other environmental toxicants, infection during pregnancy has also been shown to be associated with ASD diagnosis (Patterson, 2011). Human and animal studies have both shown that maternal immune activation leads to increased neuroinflammation in the fetus, as well as an ASD behavioral phenotype in the offspring (Estes & McAllister, 2016). The literature establishes that microglia and astrocytes release proinflammatory mediators (*e.g.*, chemokines and cytokines) in neurological pathologies like ASD (Kierdorf and Prinz, 2013). In previous studies conducted by this lab in mice, increased proinflammatory mediators and upregulation of the expression of specific transcription factors (TF) was associated with both acute and developmental exposure to

DE (Cole *et al.,* 2016; Chang *et al.,* 2019). Perinatal DE exposures of mice from E0 to PND21, using a relatively high but environmentally-relevant concentration of 250-300 $\mu g/m^3$, also generated deficits in three behavioral areas associated with ASD—social interaction and novelty, communication, and repetitive behaviors (Chang *et al.,* 2018).

There is no doubt that prevalence of ASD has grown considerably, but the debate is still out on whether that is due to better diagnosing procedures, improved definitions of ASD, growing awareness, or something more nefarious like increased air pollution. The evidence for the latter is growing; a meta-analysis that used three different statistical models to decrease the effects of confounding factors showed that perinatal exposure to $PM_{2.5}$ was associated with increased risk (7%, 5%, and 15%) of ASD in newborns regardless of the model used (Dutheil *et al.,* 2020).

1.3 Gclm knockout mouse model

Markers of genetic susceptibility have gone largely unstudied in epidemiological research regarding the CNS effects of AP. A marginal number of studies focused on AP have looked at gene-environment interactions to investigate genetic susceptibility to this neurotoxicity. An experiment conducted by Veronesi *et al.,* (2005) used an apolipoprotein E (*ApoE*)-knockout mouse model ($ApoE^{-/-}$) that was susceptible to not only neurochemical changes but also atherosclerosis, aneurysm, and ischemic heart disease—all disease outcomes for exposure to AP. Results showed that there was significant degeneration of neurons in the substantia nigra of $ApoE^{-/-}$ mice exposed to ambient particles, comparable to that seen in Parkinson's disease (Veronesi *et al.,* 2005).

Animal models, specifically certain strains of mice, have been shown to display ASD-associated behaviors and prove to be a valuable model for studying etiology and pathogenesis. In a study conducted by Gu *et al.,* glutamate-cysteine ligase (GCL) activity was shown to be reduced by 38.7% in ASD subjects (2013). GCL is the first and rate-limiting enzyme in the synthesis of glutathione (GSH) and an important participant in combatting ROS (Franklin *et al.,* 2009). GCL has a catalytic subunit (GCLC) as well as a modifier subunit (GCLM); without GCLM, GSH synthesis is reduced. GSH is a scavenger of free radicals and is used by glutathione peroxidases and transferases, as well as peroxiredoxin-6 to limit reactive aldehydes and peroxides (Costa *et al.,* 2014a). When ROS are allowed to spread uncontrollably oxidative stress occurs which leads to DNA, protein, and membrane impairment. A mouse model with decreased GSH synthesis has been shown useful in studying disorders associated with oxidative stress, like ASD. Nakamura *et al.* found that the -588T polymorphism of the human *GCLM* gene decreases its expression, resulting in increased susceptibility to oxidative stress (2002). While *Gclm*$^{-/-}$ mice have extreme decreases in GSH, this decrease appears to activate a separate compensatory pathway; thus, this model is not relevant for studying human *GCLM* polymorphisms. *Gclm* heterozygous (*Gclm*$^{+/-}$) mice are more representative of the human population and are the ideal model to study this gene-environment interaction (Franklin *et al.,* 2009; Weldy *et al.,* 2011). In studies conducted previously in our lab, *Gclm*$^{+/-}$ mice were shown to be the most susceptible to lipid peroxidation, increases of pro-inflammatory cytokines, and microglial activation when acutely exposed to DE (Cole *et al.,* 2016), as discussed in more detail in the next section. To address the importance of GSH for protecting against these effects, we used this mouse model to further examine the effects of gene-environment interactions associated AP (Cole *et al.,* 2016, 2019; Giordano *et al.,* 2006; Veronesi *et al.,* 2005; Weldy *et al.,* 2011).

1.3.1 Previous Gclm knockout evidence

Gclm$^{-/-}$ mice have been shown to be more sensitive to various toxicants of interest. Acetaminophen-induced hepatotoxicity was increased in both *Gclm*$^{+/-}$ and *Gclm*$^{-/-}$ mice when compared to wild type (WT) mice (McConnachie *et al.,* 2007). Other studies from this lab showed that neuronal cells from *Gclm*$^{-/-}$ mice were more susceptible to organophosphate insecticide toxicity, which has been shown to cause oxidative stress (Giordano *et al.,* 2007). The *Gclm*$^{-/-}$ model was also shown to be more susceptible to the effects of methylmercury, PCBs, and domoic acid (Giordano *et al.,* 2006; Costa *et al.,* 2007).

As previously described, $PM_{2.5}$ has been repeatedly associated with adverse cardiovascular and respiratory outcomes. Because of this association Weldy *et al.* exposed *Gclm* transgenic mice to DE and demonstrated that *Gclm*$^{+/-}$ mice had marked increases in lung inflammation (2012). A 2016 study conducted in our lab showed that *Gclm*$^{+/-}$ male mice (the most susceptible sex and genotype) exposed to DE were shown to have 314 pg/mL of IL-6 in hippocampal samples, a 30-fold increase when compared to the least susceptible mice (Cole *et al.,* 2016). In the absence of any toxicant exposures, the null model (*Gclm*$^{-/-}$) was also shown to have no difference from the WT mice in several behaviors associated with ASD, concluding that this deficiency alone does not lead to functional deficits without induction of oxidative stress (Cole *et al.,* 2011).

1.4 Hypothesis

Previous experiments in our lab demonstrated that perinatal DE exposure of C57Bl/6 mice was associated with behavioral deficits of the pups in three hallmark categories associated with ASD: social novelty, repetitive behaviors, and communication (Chang *et al.,* 2018). Prior publications

by Cole *et al.* have also shown biochemical changes associated with ASD after acute exposure to DE. In adult mice, it was also shown that *Gclm*$^{+/-}$ mice were particularly susceptible to the neurotoxic effects of DE exposure (Cole *et al.,* 2016). Specifically, levels of pro-inflammatory cytokines (IL-1β, IL-6, TNFα), as well as microglial activation markers (Iba1), and lipid peroxidation increased more in *Gclm*$^{+/-}$ mice than in *Gclm*$^{+/+}$ mice following acute DE exposure. Due to these findings, and to characterize GSH's role in DE toxicity, the hypothesis of the current study is that biochemical and behavioral measures associated previously with DE-induced developmental neurotoxicity will be increased in the *Gclm*$^{+/-}$ mouse model. Though both biochemical and behavioral evidence shows a clear association between perinatal DE exposure and neurotoxicity, it is unknown if these effects persist or are exacerbated in an environment with decreased GSH synthesis. Therefore, the objective of this study is to explore the role of environmental DE in the development of biochemical and behavioral changes associated with ASD in a *Gclm*$^{+/-}$ transgenic mouse model, focusing on the role of neuroinflammation. This objective was addressed using the following specific aims.

1.5 Specific Aims

Aim 1: Analysis of autism spectrum disorder-related behaviors

Due to previously seen effects of developmental DE exposure on the onset of ASD-related behaviors in mice, we explored two of the three major behavioral hallmarks of ASD: 1) repetitive behaviors, using the marble burying test and T-maze spontaneous-alternation test, and 2) social interactions, using the 3-chamber social preference test. Previous behavioral testing on *Gclm*$^{-/-}$ mice have shown that GSH deficiency alone does not induce these behavioral alterations

(Cole *et al.,* 2011). We proposed that DE-associated increases in these ASD-related behaviors would be greater in the *Gclm*$^{+/-}$ mice offspring than in *Gclm*$^{+/+}$ offspring.

Aim 2: Quantification of oxidative stress levels in the cortex following DE exposure

We chose to explore oxidative stress based on the previously described increase in brain lipid peroxidation when mice were exposed to DE, as well as GSH's known role in modulating lipid peroxidation. Oxidative stress was quantified by measuring lipid peroxidation via the thiobarbituric acid reactive substances (TBARS) assay, with an expectation of overproduction of malondialdehyde (MDA) in the presence of increased free radicals. We proposed that DE-associated increases in lipid peroxidation would be greater in the brains of *Gclm*$^{+/-}$ mice offspring than in those of *Gclm*$^{+/+}$ offspring.

Aim 3: Quantification of proinflammatory cytokine production, microglial activation markers, and proteins associated with dysregulated neurodevelopment

Based on previous DE-induced differences found in inflammatory-associated markers (IL-1β, IL-6, TNFα, IL-4, and STAT6) and PAX6 (associated with disrupted neurogenesis) this aim used quantification of mRNA expression of these markers in addition to select others via real-time quantitative polymerase chain reaction (qRT-PCR) analysis (Sakurai & Osumi, 2008). Because previous findings from our lab regarding these specific changes were generally found in the cortex of mice, we chose to isolate these measurements to that region of the brain. STAT1 was measured because of its known implication in inflammatory mediation as well as previous findings by Li *et al.,* showing that it was decreased in ASD associated neural progenitor cells (NPCs), indicative of axonal sprouting dysfunction (Li *et al.,* 2021; Kaplan 2013). In addition,

IFNγ was quantified due to associations found in a systematic review by Masi *et al.,* (2015) between ASD and a chronic state of cytokine induction via pathways known to be modulated by IFNγ as well as TNFα. Of the markers quantified by qRT-PCR, total protein levels were measured via enzyme-linked immunosorbent assay (ELISA) for IL-1β, IL-6, TNFα, IL-4, and IFNγ to corroborate results. PAX6 protein was measured via Western blot (WB) analyses. We proposed that these inflammatory-associated changes would be exacerbated in the brains of *Gclm*$^{+/-}$ mice.

Microglia have been previously shown as particularly sensitive to environmental changes and have vital roles in brain development. Specifically, a suspected precursor to the increase of cluster of differentiation 68 (CD68) in the prefrontal cortex, 4-methylphenol (p-Cresol), was found to be elevated in fecal samples from children diagnosed with ASD (Davoli-Ferreira *et al.,* 2021). Cole et al. (2016) demonstrated that increased microglial activation was found after acute exposure of adult mice to DE. To extend these results to developmental exposures, as well as explore the effects in a *Gclm*$^{+/-}$ mouse model, this aim examined mRNA levels of the microglial activation markers *Iba1* and *Cd68* via qRT-PCR, and total protein was verified for IBA1 via WB. Microglial activation was also expected to be exacerbated in the *Gclm*$^{+/-}$ mice compared to *Gclm*$^{+/+}$ mice.

Materials and Methods

2.1 Materials

TBARS Assay Kit and RIPA buffer concentrate (50 mM Tris HCl pH 8, 150 mM NaCl, 1% NP-40, 0.5% sodium deoxycholate, 0.1% SDS) were purchased from Cayman Chemical (Ann Arbor,

MI, USA). XCell II Blot Module, XCell SureLock Electrophoresis Cell, NuPAGE MOPS SDS Running Buffer 20x, NuPAGE LDS Sample Buffer 4x, NuPAGE Antioxidant, NuPAGE Sample Reducing Agent 10x, and NuPAGE 10% Bis-Tris Protein Gels were purchased from Life Technologies (Carlsbad, CA, USA). Immobilon-P Transfer Membrane was purchased from Millipore Corporation (Billerica, MA, USA). BCA Protein Assay Kit, Interleukin 4 (IL-4) Mouse ELISA Kit, IL-6 High Sensitivity Mouse ELISA Kit, IL1-β Mouse ELISA Kit, IFNγ Mouse ELISA Kit, TNFα Mouse ELISA Kit, Restore Western Blot Stripping Buffer, PageRuler Prestained Protein Ladder, Pierce Protease Inhibitor Mini Tablet (EDTA-free), and SuperSignal West Pico Chemiluminescent Substrate were purchased from Thermo Fisher Scientific (Waltham, MA, USA). Anti-ionized calcium-binding adapter molecule 1 (IBA1) antibody was purchased from Abcam (Boston, MA, USA). Anti-paired box 6 (PAX6) antibody and Anti-β-actin antibody was purchased from MilliporeSigma (Burlington, MA, USA). Anti-rabbit IgG HRP-linked antibody was purchased from Cell Signaling Technology (Danvers, MA, USA). RNeasy Mini Kit was purchased from Qiagen (Hilden, Germany). iScript cDNA Synthesis Kit, iTaq Universal SYBR Green Supermix and CFX384 Real-Time Detection System were purchased from Bio-Rad Laboratories (Hercules, CA, USA). All qPCR primers were purchased from Integrated DNA Technologies (Newark, NJ, USA).

2.2 Animal and tissue preparation

All procedures were conducted in accordance with the National Institute of Health Guide for the Use and Care of Laboratory Animals and were approved by the University of Washington Institutional Animal Care and Use Committee (Institute for Laboratory Animal Research (U.S.), 2011; PROTO201600548).

2.2.1 Mice

Throughout breeding, the animals were housed at the University of Washington Controlled Exposure Laboratory's Northlake Diesel Facility (Seattle, WA). They were brought to the facility 1 week before breeding for acclimation and received filtered air (FA) or DE for the duration of their stay. For the study, 120 8-week-old C57Bl/6J females (WT) purchased from Jackson Laboratory were time-mated (2 females-1 male) to $Gclm^{+/-}$ male mice (Botta *et al.,* 2008; Franklin *et al.,* 2009). The $Gclm^{+/-}$ mouse model was generated in-house and backcrossed to B6 as previously described (Franklin *et al.,* 2009). $Gclm^{+/-}$ males used as sires for the timed mating were produced by crossing $Gclm^{+/-}$ and $Gclm^{+/+}$ males and females. Mice were housed in specific-pathogen-free facilities at the University of Washington, on a 14 h light-10 h dark cycle with *ad libitum* access to standard mouse chow and water. For genotyping purposes, DNA from ear punch tissue was isolated by Qiagen DNeasy kit according to manufacturer's instructions and analyzed via PCR amplification.

2.2.2 Diesel exhaust (DE) characterization

To resemble environmental diesel emissions, the University of Washington's (UW) Northlake Controlled Exposure Facility runs a two-stage exhaust-dilution diesel generator engine, operated under load and with feedback control (Gould *et al.,* 2008). This single-cylinder 5.5-kW generator (Yanmar model YDG5500EV-^EI) allows for dynamic control of $PM_{2.5}$ concentration (Fig. 2.1). A diesel fuel with low sulfur content (15 ppm) is used to imitate current highway grade (#2) diesel fuel. The load bank is set to control the load (1.5kW, low-4.5kW, high) (Simplex Model Swift-E FT, Springfield IL). While the system allows for exhaust to be irradiated for generation of O_3, this feature was not utilized for the current study. The DE characteristics are intensely

influenced by the load that the engine is run under. A higher load of 70-80% is most relevant for our exposures (Fox *et al.,* 2015). Exposure in this facility allows for repeatable exposures with consistent concentration across groups. (Gould *et al.,* 2008).

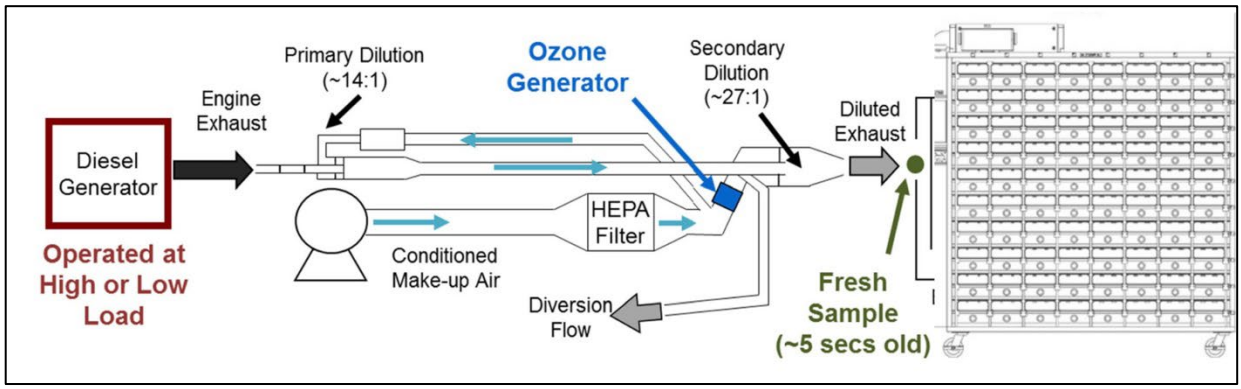

Figure 2.1 Diesel exhaust system schematic Fox et al., 2015. *System simulates dispersion of atmospheric DE by generating exhaust from the center of the pipe through the muffler under (+) pressure into a dilution system. The 1 ° DE exhaust mixture then moves through the dilution pipe and is mixed with HEPA-filtered air to the desired concentration. This then enters the intake to produce a uniform flow that is then distributed to the air intake of a standard Allentown mouse housing rack.*

The following composition and particle size characterization for this facility were found in a supplementary comparison of the newer Yanmar vs. the replaced Cummins engine (Fox *et al.,* 2015; Gould *et al.,* 2008). Size distribution was comparable to ambient diesel particles ~100 m away from major roadways. $PM_{2.5}$ size was measured with a micro-orifice uniform deposition impactor (MOUDI) and found to have a median aerodynamic diameter of 77 nm, representative of a population containing mostly fine particulate matter (Yin *et al.,* 2013). Species composition from the Yanmar generator yielded mass fractions of 1.03 µg/µg for elemental carbon (EC) and 0.10 µg/µg for organic carbon (OC), a ratio of 0.10 lower than previous estimates in Gould *et al.,* 0.34 (2008). The NO_2 composition (measured by chemiluminescence) was an average 190 ppb; because of lack of sunlight the NO_x remained mostly as reduced NO with a concentration of 1,160 ppb. CO_2 measured 790 ppm with CO concentrated at 1.34 ppm. The concentration of particle-bound PAH was 21 ng/µg while nitrated-PAH (as represented by 1-nitropyrene

concentration) was 0.14 pg/µg. Dithiothreitol reactivity is a measurement of the ability of PM to produce reactive oxygen species (ROS) and was found to be, on average, 145 ng/min/m^3, approximately 10 times higher than the average found from six urban areas in the U.S. (Vedal *et al.,* 2013). Finally, the mass fraction for all metals was between 0.001-0.00001 (Fox *et al.,* 2015).

2.2.3 Diesel exhaust exposure

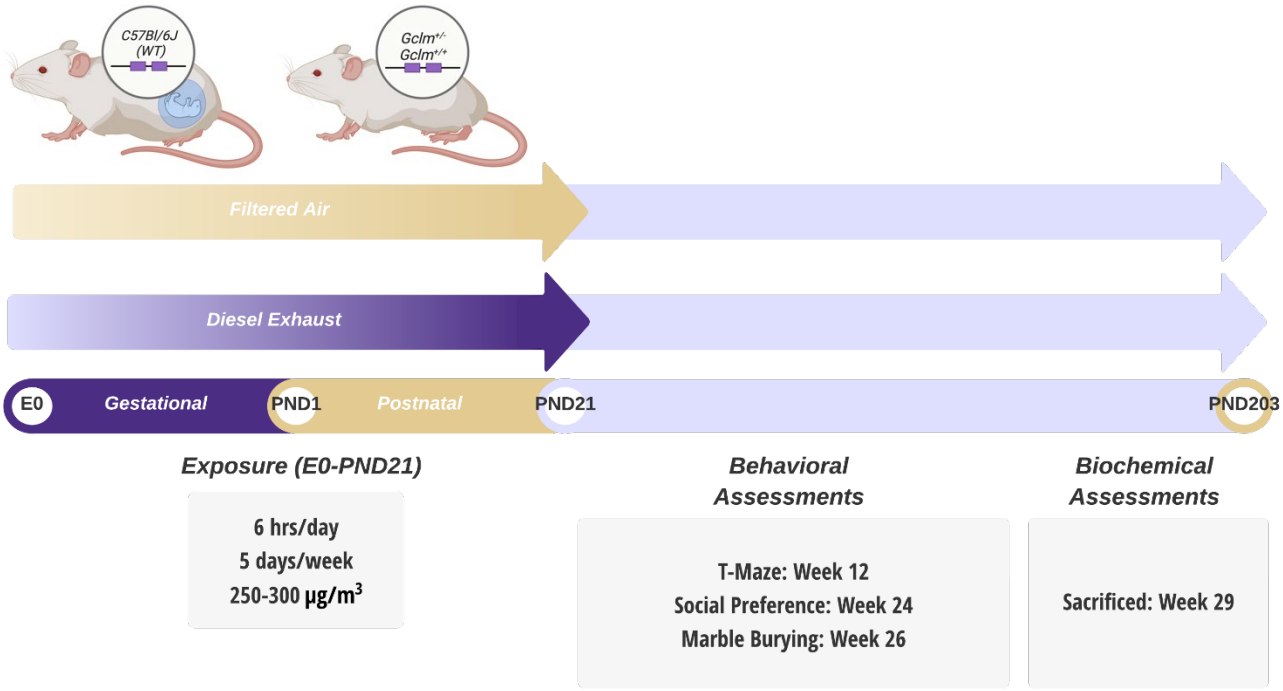

Figure 2.2 Exposure paradigm. *A total of 120 C57Bl/6 (WT) females were time-mated with 40 Gclm$^{+/-}$ males and exposed from E0-PND21 to 250-300 µg/m^3 for 6 h a day, 5 days a week. Behavioral assessments were conducted on the following timeline: T-maze at 12 weeks, social preference at 24 weeks, and marble burying at 26 weeks. Mice were sacrificed at 29 weeks and biochemical endpoints related to inflammation, microglial activation, and oxidative stress were assessed.*
Created with: Biorender, Lucidchart (www.lucidchart.com).

Mice were brought to the NLD vivarium 1 week prior to breeding for acclimation, then 120 8-week-old C57Bl/6J (WT) females were time-mated with 40 *Gclm*$^{+/-}$ males and assessed the next morning (E0) for the presence of vaginal plugs. On E0, plug-positive females were transferred to individual cages in either the DE or FA rack for exposures from E0 – PND21. The C57Bl/6 dams

(and their *Gclm*$^{+/+}$ and *Gclm*$^{+/-}$ offspring) were exposed perinatally, for a total of 41 days, from ages E0 to PND21 to 250-300 μg/m^3 $PM_{2.5}$ concentration of DE at the UW Controlled Exposure Laboratory located in the Northlake Diesel Facility (Seattle, WA). DE was generated under 70% electrical load as described above (Gould *et al.,* 2008; Fox *et al.,* 2015). A two-step dilution system was used to pass DE from the generator continuously with a controlled concentration of $PM_{2.5}$ of 250-300 μg/m^3, which was monitored with an in-cage nephelometer. This diluted DE was transferred through a ductwork system to the air intake of a mouse housing rack (Allentown) which distributed the diluted DE equally to all cages in the rack. Control mice were housed in a separate rack and exposed to filtered air (FA), the same HEPA- and carbon-filter purified air that was also used for dilution of the DE to its target concentration (Fig. 2.1). After PND21, mice were weaned and transferred to a different centralized UW vivarium where they were housed in ventilated racks. Mice were group-housed for the duration of the experiment, with 2 to 5 same-sex littermates housed per cage.

2.3 Behavioral testing

Following DE exposures, mice were transferred to the UW T-wing vivarium, where the UW Center on Human Development and Disability (CHDD)'s Mouse Behavior Laboratory is located and were housed until sacrificed. Same-sex siblings were housed together. A variety of behavioral tests were used, focusing on impairment of hallmark behaviors typically affected in ASD—deficits in social interaction and the occurrence of repetitive behaviors. For each test described below, 20 male and 20 female mice were used per exposure group (DE and FA) and genotype (*Gclm*$^{+/+}$ & *Gclm*$^{+/-}$) at either 12, 24, or 29 weeks of age. The selected age of the mice was initially intended to mimic behavioral testing based on Chang *et al.*, (2018); however, due to

restrictions related to the COVID-19 public health emergency we were unable to keep this testing timeline. All behavioral testing was recorded with Ethovision® XT video tracking system purchased from Noldus Information Technology (Wageningen, Netherlands) and was scored by a trained individual blinded to treatment and group assignment.

2.3.1 T-Maze for spontaneous alternation

The T-Maze spontaneous alternation test is commonly used to evaluate working memory as well as repetitive behaviors in mice. Typically, exploratory drive urges mice to explore different parts of the maze, leading them to spontaneously alternate which arm they choose to enter. This spontaneous alternation occurs in most strains of mice and is partially controlled by hippocampus-dependent spatial working memory. In mice that exhibit repetitive behaviors, as seen in mouse models of ASD, they will display an increased penchant for repetitive entries to the same arm (Ye *et al.,* 2016). Mice (*n*=20 per treatment group, sex, and genotype) were evaluated at 12 weeks of age using a continuous alternation T-Maze protocol arm (Chang *et al.,* 2018). The three arms were placed in a T-formation on a 57 cm table (Fig. 2.3) and light emitted in the start arm

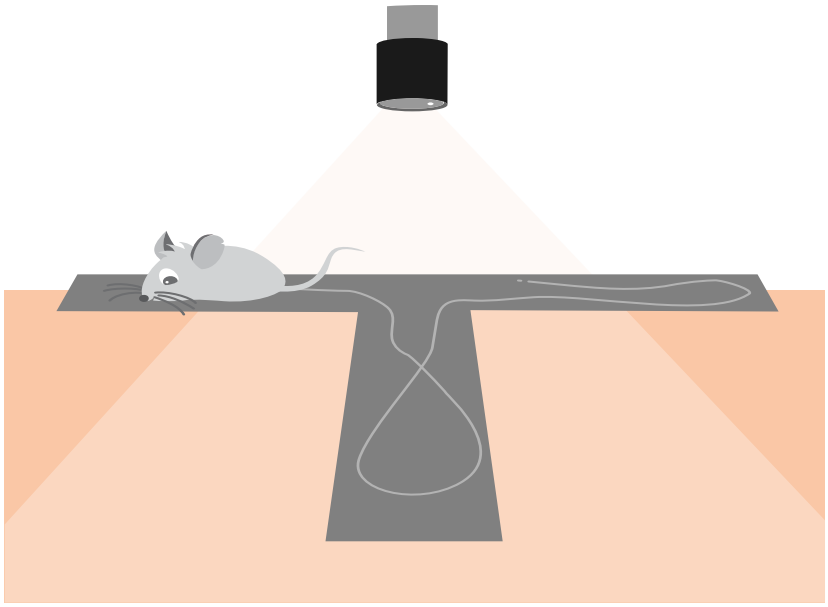

Figure 2.3 T-maze for spontaneous alternation. *T-maze was composed of three 31 cm x 11.5 cm x 21 cm arms connected by a 10 cm x 10 cm center and customized guillotine doors. This assessment is used to assess repetitive behaviors associated with ASD in mice.*
Source: Noldus

as well as the 2 goal arms was measured at 250-300 lumens. The evaluation began with one forced-side trial followed by 14 free-choice trials. During the first trial, one goal arm was blocked at random by the guillotine door. The mouse was blocked at the distal 1/3 end of the start arm for 10 s. To start, the trial the door was then raised, and the mouse was allowed to enter the unblocked arm. The mouse then returned to the start arm where they were blocked for 10 s to start the next 14 free-choice trials. For each of the 14 free-choice trials, they were allowed to enter whichever arm they choose. Once they completely entered a goal arm, they were blocked in the chosen arm for 15 s, while the un-chosen arm was blocked. After the time elapsed, they were able to return to the start and subsequent trials were performed. Video tracking with EthoVision XT (Noldus) was used to record each session from above. Calculation of the percentage alternation was performed by the following equation:

$$\frac{\text{\# of times entered alternating arms}}{\text{total free-choice trials}}$$

If the subject's tail tip entered a specific arm, that was considered an entry. Analysis was completed blinded to the exposure groups.

2.3.2 Marble burying task for repetitive and persistent behaviors

The marble burying task has been utilized extensively to assess repetitive and persistent behaviors, particularly for ASD mouse models. Interestingly, increased repetitive behaviors in this test are also seen in the maternal immune activation (MIA) model of ASD (Ye *et al.,* 2016). This repetitive digging behavior was evaluated via the marble-burying task protocol described previously (Chang *et al.,* 2018). At 26 weeks of age, mice (n=20 per treatment group, sex and genotype) were positioned in the cage filled with 5 cm of shaved bedding with 12 blue marbles spaced equally as a 3 x 4 grid on the bedding (Fig. 2.4). The number of marbles that are buried is

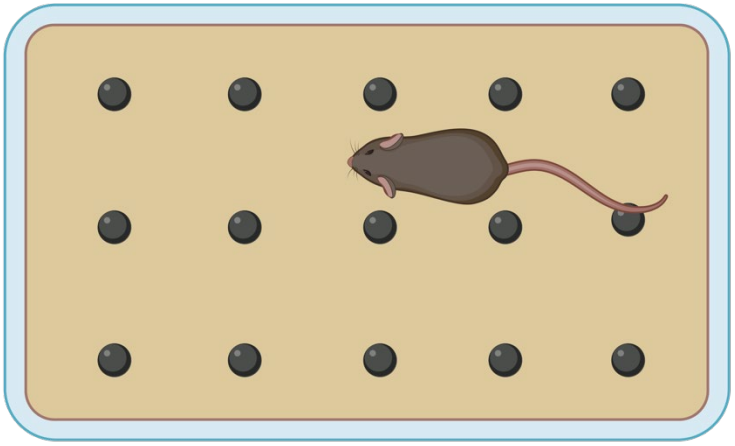

Figure 2.4 Marble burying task for repetitive behaviors. *The marble burying assessment utilized a clean standard housing cage, measuring 484 cm^2, filled with 5 cm shaved aspen bedding, 12 blue marbles of 1.58 cm diameter, and a clear acrylic ceiling with ventilation holes. The task is used to assess both repetitive and persistent behaviors in mice.*
Source: Created with BioRender.

used as a measurement for repetitive digging behavior (see Materials). Four mice were tested simultaneously, using 4 cages arranged in a 2 x 2 grid, with a clear acrylic ceiling with ventilation holes placed over the cages, and a camera placed overhead to record each trial (EthoVision XT, Noldus). Ceiling, cages, and marbles were cleaned and dried between each subject. For our purposes, marbles were considered "buried" when the marble was more than 2/3 covered. Analysis was completed by scoring video footage every 5 min, with the scorer blinded to exposure group and marble number.

2.3.3 Three-chambered social preference test for social novelty and sociability

The three-chambered social preference test is the most used assessment to measure social novelty and sociability in ASD mouse models (Chang *et al.,* 2018). It evaluates sociability by measuring time spent with another mouse as well as the mouse's ability to choose between acquainted and novel mice. A social preference test from Chang *et al.,* was modified and the mice were evaluated at 24 weeks of age (2018). Sociability for our purposes is defined as preferential interaction with mouse "N1" versus an "empty" cage while social *novelty* is defined

as preferential interaction with a novel mouse "N2" versus N1. A three-chambered clear box with a video camera recording from above (see Materials) was used for the testing procedure, which was structured in three phases—habituation, sociability, and social novelty. The testing began with habituation, where the test animal (n=20 per treatment group) was put in the middle chamber with an empty cup in each side chamber and allowed to freely explore for 10 min. Sociability was then evaluated by placing an age- and sex-matched mouse (N1) into one of the cups; the test animal was then allowed to explore for 10 more min. Finally, social novelty was tested by putting an additional mouse (N2) in the other cup, and the test animal was again allowed to freely explore for 10 min. Sociability was assessed by measuring the time (s) interacting with the cup holding N1, as compared to the empty cup. "Interaction" was defined as nose-tip of the test animal being in the cup's "zone", which was a 2 cm radius around the cup. Social novelty was analyzed by measuring the time (s) the test animal interacted with the cup holding N2, as compared to the cup holding N1. The interaction data was automatically analyzed by Ethovision® XT 15 software.

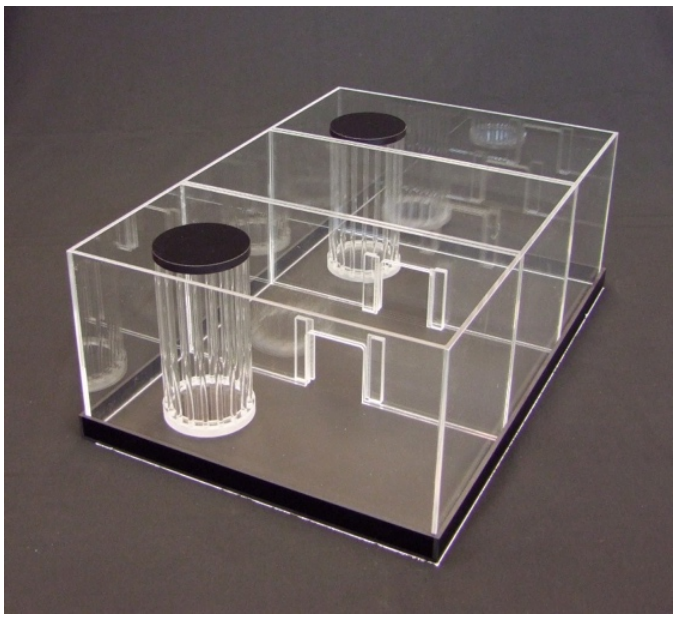

Figure 2.5 Social preference test. *Social novelty and sociability was tested using a three-chambered clear acrylic box with chambers measuring 20 cm x 40 cm x 22 cm in size with spacing in between the openings. Two metal restraining cups (11 cm h x 10.5 cm d) with bars at 1 cm interval spacing were used for tactical interaction. Ethovision® XT video tracking system purchased from Noldus Information Technology (Wageningen, Netherlands) was used for automated analysis purposes. This set up was used to test both sociability and social novelty in mice.*
Source: Noldus.

2.4 Biochemical endpoints

2.4.1 Tissue collection

Mice were sacrificed at 29-weeks-old by CO_2 asphyxiation and the brain was collected; brain regions (olfactory bulb, cortex, striatum, hippocampus, and cerebellum) were freshly dissected and immediately frozen in liquid nitrogen as described (Spijker, 2011). The tissue was ground with a pre-chilled mortar and pestle and stored at −80°C for later use. Cortex was used for all biochemical endpoints in this study.

2.4.2 Immunoblot

Paired Box 6 (PAX6) and Ionized calcium binding adaptor molecule 1 (IBA1) protein levels (*n*=5-6 mice per treatment group) were measured using Western blot. Immunoblots were completed with a modified protocol as previously described (Garrick *et al.,* 2016). Mouse cortex samples were prepared by adding previously powdered tissue in 10X RIPA buffer and protease inhibitors (see Materials). Completion of homogenization was performed on samples of ground tissue; first manually with a 20G needle then via sonication. To determine protein content for samples, a Pierce™ Bicinchoninic Acid (BCA) assay was conducted with bovine serum albumin (BSA) as a standard according to manufacturer's protocol (Thermo Fisher Scientific, 2020) before samples were prepared for sodium dodecyl sulfate-polyacrylamide gel electrophoresis (SDS-PAGE). Twenty (20) μg of protein was added to SDS running buffer and reducing agent and loaded on a pre-made 10% Bis-Tris polyacrylamide (PAGE) gel and run at 30 mA for 45 min followed by 60 mA for 90 min. After electrophoresis was completed, proteins were transferred from the PAGE gel to polyvinylidene difluoride membranes at 4°C for 1000 mA total (*e.g.* 16 hours at ~63 mA). The membrane was then blocked for 1 h in BSA blocking agent (powdered milk) and probed with primary antibodies using the following dilutions—PAX6

(1:5000 overnight at 4°C on shaker); IBA1 (1:1000 overnight at 4°C no shaker). After probing with primary antibody, membranes were washed with tris-buffered saline and 0.1% Tween-20, pH=7.5 (TBST), then probed with horseradish peroxidase-conjugated anti-rabbit secondary antibody at 1:5000 dilution for 1 h at room temperature (RT). Membranes were then developed and visualized using a chemiluminescent substrate in HOPE MicroMax X-ray processor. Following visualization, the membranes were stripped using Restore™ Stripping Buffer and re-probed with primary β-actin antibody (housekeeping protein) at a dilution of 1:2500 for 20 min at RT followed by horseradish peroxidase-conjugated anti-mouse secondary antibody at dilution 1:5000 for 20 min at RT. Intensity of bands was measured via densitometric analysis using ImageJ software (NIH), where the PAX6 and IBA1 band intensities were normalized to β-actin expression.

2.4.3 Enzyme-linked immunosorbent assay (ELISA)

Mouse protein levels of the cytokines IL-4, IL-6, IL-1β, IFNγ, and TNFα were measured via Invitrogen ELISA kits (see Materials). Mouse cortex samples were prepared by adding 20-50 mg frozen cortex powder in 5M guanidine-HCL pH 8.0 lysis buffer, sonicated as described previously, and stored at -80°C for future use. Homogenates were diluted in cold PBS buffer as follows for each target—undiluted (IL-6, TNFα), 1:9 (IL-4, IL-1β), and 1:7 (IFNγ), with addition of protease inhibitors. For IL-6 and IL-4 only, the samples were further diluted 1:1 in provided ELISA diluent before the assay was conducted. ELISAs were conducted according to manufacturer's protocol (Invitrogen, Waltham, MA, USA) and normalized to total protein in each sample as measured by BCA Assay (Thermo Fisher Scientific, Waltham, MA, USA) using BSA as standard.

2.4.4 Real-Time quantitative reverse transcription-PCR (RT-qPCR)

RNeasy Mini Kit (see Materials) was employed to extract total RNA from cortex samples according to manufacturer's protocol. iScript cDNA Synthesis kit (Bio-Rad Laboratories, Hercules, CA) was utilized to generate cDNA from 1µg of total RNA according to manufacturer's protocol. Cortex cDNA samples were diluted to 6.25 ng/µL in nuclease-free H_2O; these samples were used for real-time quantitative polymerase chain reaction (RT-qPCR) via iTaq Universal SYBR Green Supermix in a CFX384 Real-Time Detection System (see Materials). A master mix was made with 6 µL of sample, 15 µL 2X SYBR Green Supermix, 1.5 µL 10 µM forward primers, 1.5 µL 10 µM reverse primers, and 6 µL nuclease-free H_2O (total volume of 30 µL). Each sample was then run (in triplicate) under the following conditions—denatured 95°C for 30 s, 40 cycles at 95°C for 15 s, 60°C for 30 s, and a last 30 s step at 72°C. RT-qPCR was utilized to measure mRNA levels of the following targets—inflammation targets (*Il-4, Il-6, Il-1β, Ifnγ, Tnfα, Stat, Stat6*), microglial activation target *Cd68*, and ASD associated target *Pax6* (see Appendix for primer pair sequences). Relative mRNA (delta quantitative cycle, dCq) was calculated for each target by subtracting the Cq values of *Gapdh* (housekeeping gene) from the target Cq value.

2.4.5 Thiobarbituric acid reactive substances (lipid peroxidation)

Mouse cortex samples were prepared by homogenizing previously powdered tissue in 10X RIPA buffer with protease inhibitors (see Materials). Levels of MDA were quantified via Thiobarbituric Acid Reactive Substances (TBARS) Assay Kit following manufacturer's protocol (Cayman Chemical, 2017). MDA is an end-product of lipid peroxidation which is indicative of oxidative stress. Total protein was measured via BCA Assay Kit with BSA as a standard and

completed according to manufacturer's protocol. The brain samples for the TBARS assay were diluted to a concentration of 1 μg/μL, using 100 μL of diluted samples for the assay.

2.5 Statistical Analysis

All data are expressed as the mean ± SEM. Data were analyzed via GraphPad Prism software (Version 9.3.1 (350), GraphPad Software Inc., San Diego, CA, USA). Statistical analyses for the behavioral and biochemical assessments were conducted on parametric data by one- or two-way ANOVA and Šidák correction for multiple comparisons. Birth outcome was analyzed via Fisher's exact test.

Results

3.1 Birth outcome

	Filtered air (FA)	**Diesel exhaust (DE)**
Birth outcome $(\frac{\text{plug positive F gave birth}}{\text{total plug positive F}})$	$\frac{34}{52}$ (65.4%)	$\frac{32}{59}$ (54.2%)
Survival to PND7	$\frac{226}{246}$ (91.9%)	$\frac{208}{231}$ (90%)
Sex Distribution $(\frac{\text{Male}}{\text{Female}})$	$\frac{117}{109}$ (1.07)	$\frac{98}{110}$ (0.89)
Genotype Distribution $(\frac{\text{Heterozygous}}{Total})$	$\frac{69}{157}$ (43.9%)	$\frac{50}{158}$ (31.6%)

Table 3.1 Birth outcome. *Birth outcome is shown by number of plug positive females that gave birth divided by the total number of plug positive females in both treatment groups, filtered air (FA) and diesel exhaust (DE). Further analysis showed pup survival to post-natal day 7 (PND7), sex distribution male/female, and genotype distribution HZ/WT. Measured by Fisher's exact test. WT: $Gclm^{+/+}$ HZ: $Gclm^{+/-}$.*

Previous results from this lab showed no significant differences in birth outcomes following DE exposure (Chang *et al.,* 2018). These results persisted in the current study, showing that DE

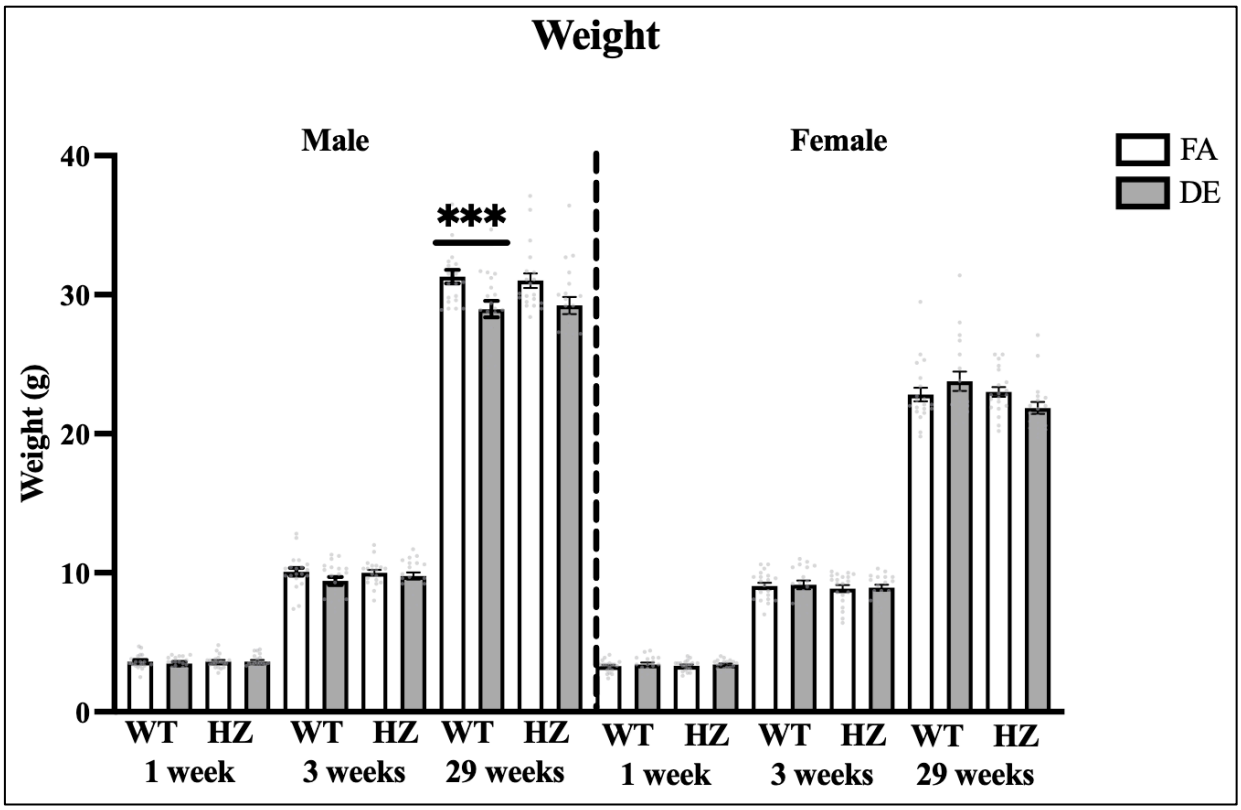

Figure 3.1 Body weight outcomes. A. *Weight (g) of male pups at 1 week, 3 weeks, and 29 weeks of age. N=20 per group. Week 29 treatment effect by two-way ANOVA and Šidák correction for multiple comparisons *** $p<0.001$.* ***B.*** *Weight (g) of female pups at 1 week, 3 weeks, and 29 weeks of age. N=20 per group, interaction effect by two-way ANOVA and Šidák correction for multiple comparisons * $p<0.05$. Error bars represent mean +/- SE. WT: $Gclm^{+/+}$ HZ: $Gclm^{+/-}$*

exposure did not affect pregnancy rate, litter size, survival rate, sex distribution, or genotype distribution (Table 3.1). A total of 52 plug-positive female mice received FA while 59 mice received DE for the length of their pregnancy (19-20 days). Thirty-four mice from the FA group gave birth (65.4%) while 32 from the DE group gave birth (54.2%) (p=0.2513 Fisher's exact). Of these pups, 91.9% (226/246) in the FA group survived to PND7 while 90% (208/231) from the DE group survived (p=0.5248 Fisher's exact).

Mice were weighed at 1 week, 3 weeks (at weaning), and 29 weeks of age (at sacrifice). In previous experiments (Chang *et al.,* 2018, 2019), body weights were unaffected by exposure.

Similarly, in the current study no differences in body weights were found at 1 or 3 weeks for either sex. However, in the current study, DE-exposed male mice of both genotypes had lower weights at 29 weeks of age when compared to the FA group. Though the change in WT weight was significant (p=0.0004 by 2-Way ANOVA), the $Gclm^{+/-}$ weights trended downward but the change was not significant (p=0.0514 by 2-Way ANOVA). In female mice, a small trend towards decreased weight was seen in DE-treated $Gclm^{+/-}$ mice, but this trend was not statistically significant (Fig. 3.1).

3.2 Exploratory drive, sociability, and repetitive behaviors

Previously established results from T-maze analysis in this lab showed that repetitive behaviors were increased with developmental DE exposure (Chang *et al.,* 2018). In the current study, ASD related repetitive behaviors were measured via spontaneous alternation in a T-Maze as well as via the marble burying test. Consistent with the previous study, DE-exposed WT males showed increased repetitive behaviors in the T-maze test, as indicated by a significant decrease in

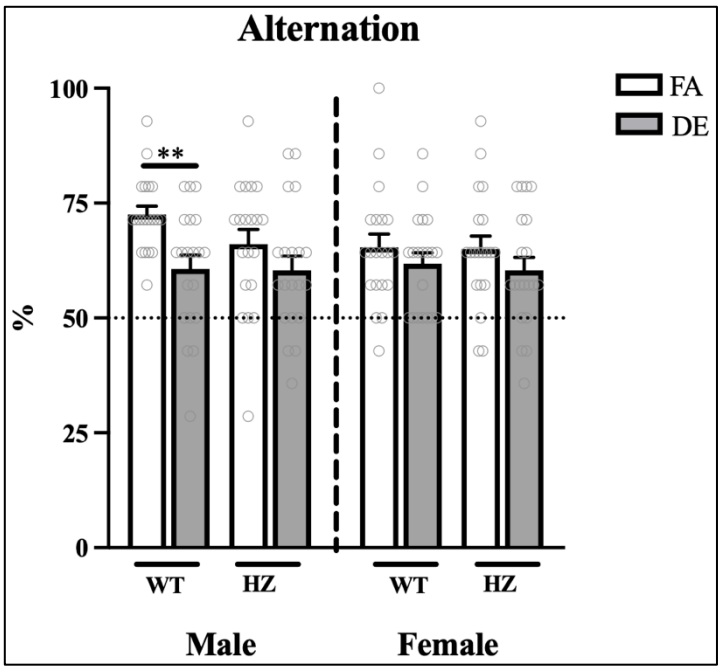

Figure 3.2 Spontaneous alternation by T-Maze. *Percent alternation in T-Maze measured at 26 weeks. N=20 per group. DE exposure was associated with a significant decrease in alternation in WT males (**p<0.01, one-way ANOVA and Šidák correction for multiple comparisons). Error bars represent mean +/- SE. WT: $Gclm^{+/+}$ HZ: $Gclm^{+/-}$*

alternation compared to FA controls (p=0.0085 by 1-Way ANOVA) (Fig. 3.2). Unlike previous studies, DE-exposed mice did not exhibit any increase in repetitive/perseverative behaviors compared to FA-exposed mice in the marble burying test (Fig. 3.3). The number of marbles buried was similar among mice of different treatment groups and genotypes.

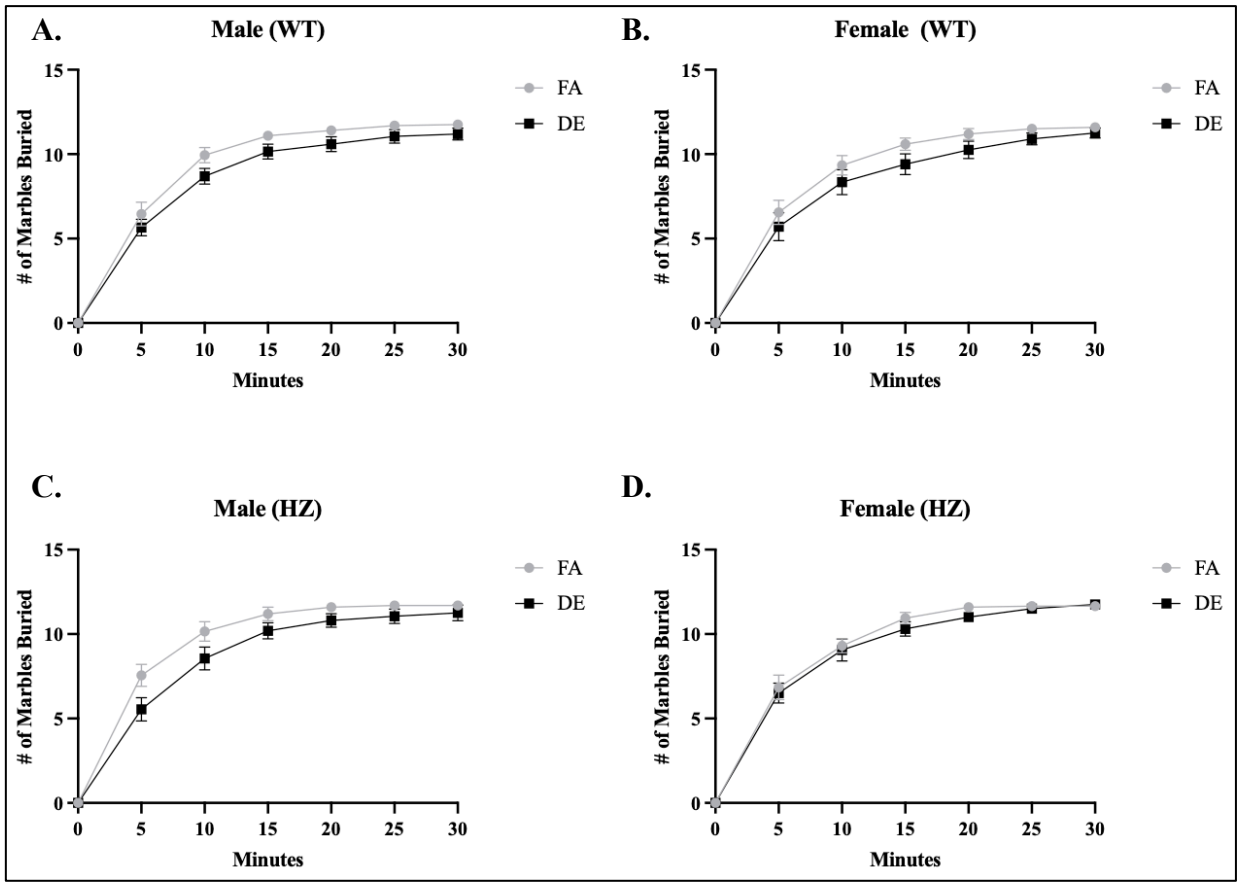

Figure 3.3 Repetitive behaviors by marble burying. *Number of marbles buried at 5 min intervals, for a total of 30 min. measured in* ***A.*** *$Gclm^{+/+}$ males* ***B.*** *$Gclm^{+/+}$ females* ***C.*** *$Gclm^{+/-}$ males* ***D.*** *$Gclm^{+/-}$ females N=20 per group, all measures not significant (ns) p>0.05 by two-way repeated measures ANOVA. Error bars represent mean +/- SE.*

Sociability and social novelty were tested using the three-chamber social preference test (Chang *et al.,* 2018). Social preference was tested in two phases. The first phase was sociability (Fig. 3.4), as measured by time spent in the chamber with an empty cup (Empty) versus time spent with a novel mouse (N1). The second phase, social novelty (Fig. 3.5), was measured by time spent with the *now* familiar mouse (N1) versus time spent with a novel mouse (N2). Comparable

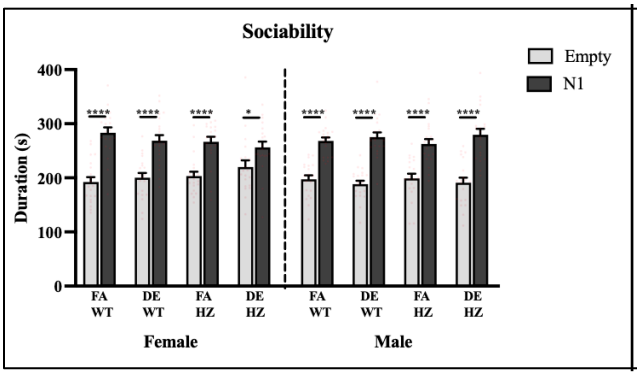

Figure 3.4 Sociability by three chamber social preference testing in male and female mice. *Time (s) interacting with empty cup (EMPTY) and cup containing novel mouse (N1), N=20 per group, ****p<0.0001, *p<0.05 by one-way ANOVA and Šidák correction for multiple comparisons. Error bars represent mean +/- SE. WT: Gclm$^{+/+}$ HZ: Gclm$^{+/-}$*

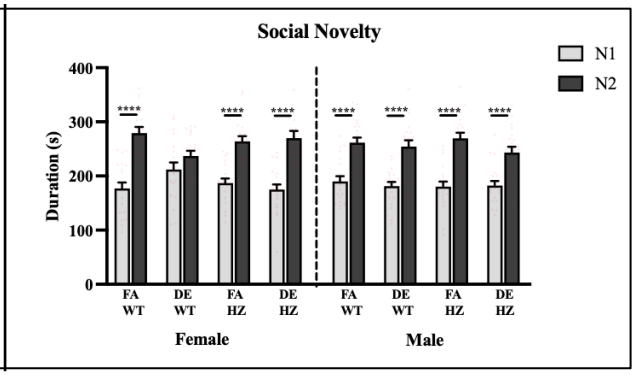

Figure 3.5 Social novelty by three chamber social preference testing in male and female mice. *Time (s) interacting with cup containing familiar mouse (N1) and cup containing novel mouse (N2), N=20 per group, an effect of treatment in WT females (N1 & N2 time difference not significant), ****p<0.0001 by one-way ANOVA and Šidák correction for multiple comparisons. Error bars represent mean +/- SE. WT: Gclm$^{+/+}$ HZ: Gclm$^{+/-}$*

to what was seen previously, our studies showed normal sociability in all groups with all mice preferring interaction with N1 versus the empty cup (Fig. 3.4). Social novelty results were also confirmed, deficits were seen in the current study with DE-treated WT females showing no preference between N1 and N2 (p<0.0001 by One-Way ANOVA) (Fig 3.5). Social novelty in the DE-treated males were unaffected; similarly, to the FA-treated mice, they preferred the novel N2 mouse over the familiar N1 mouse. Surprisingly, this effect of DE on social novelty in females was not seen in the *Gclm*$^{+/-}$ mice. Female and male *Gclm*$^{+/-}$ mice exposed to DE showed a normal preference for the N2 novel mouse over the N1 familiar mouse (Fig. 3.5). Thus again, the *Gclm*$^{+/-}$ mice were not any more sensitive to the effects of DE exposure. Indeed, in the case of social novelty they were more resistant than WT mice to the effects of DE.

3.3 Inflammatory marker expression and oxidative stress in cortex of mice

As previously established, neuroinflammation is an important proposed mechanism of developmental neurotoxicity associated with DE exposure. Earlier studies found exposure-

related differences in both transcript (*Il-1β, Il-6, Tnfα, Il-4, Ifnγ, Stat1, Stat6*) and protein (IL-1β,

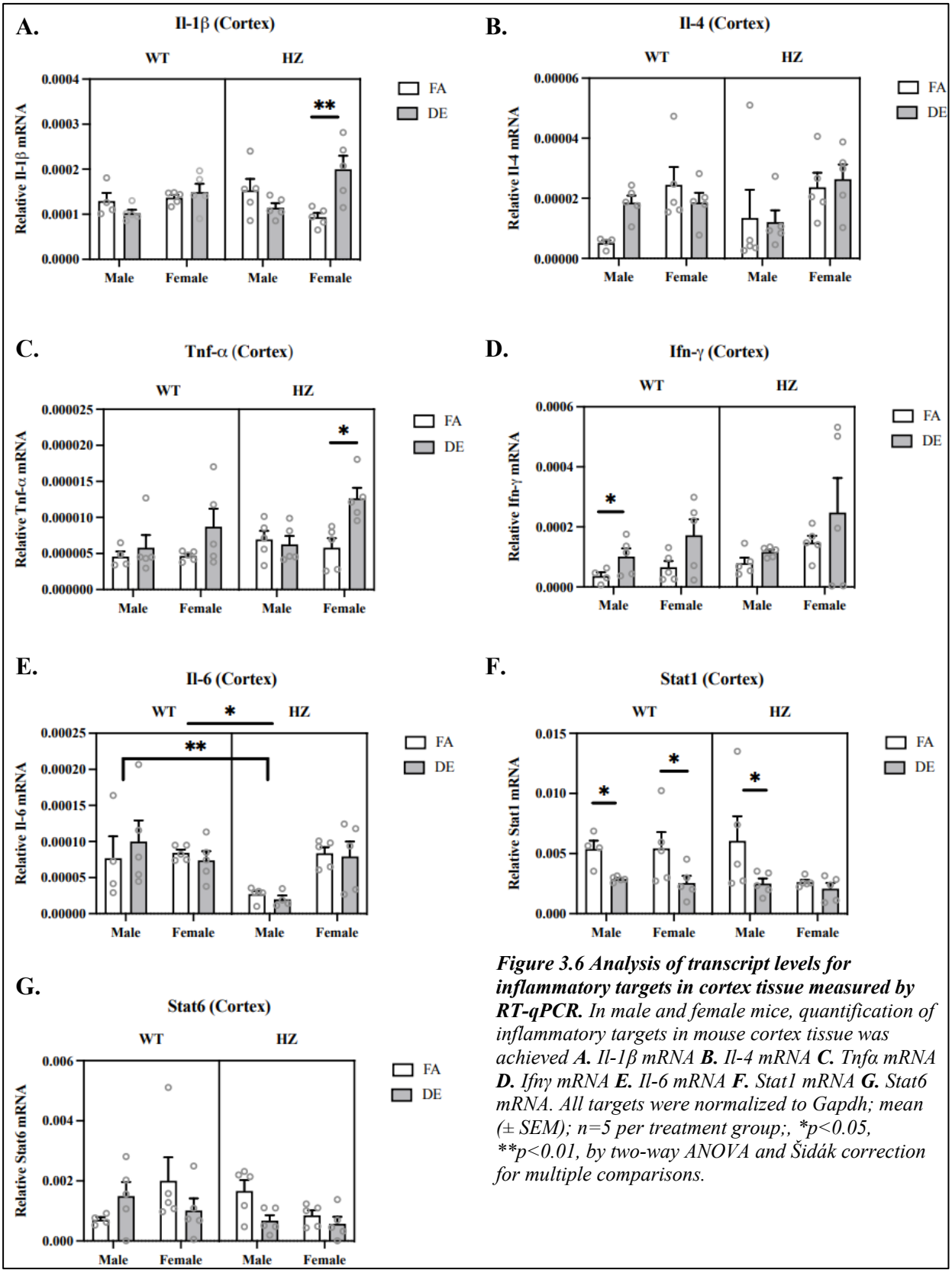

Figure 3.6 Analysis of transcript levels for inflammatory targets in cortex tissue measured by RT-qPCR. *In male and female mice, quantification of inflammatory targets in mouse cortex tissue was achieved* ***A.*** *Il-1β mRNA* ***B.*** *Il-4 mRNA* ***C.*** *Tnfα mRNA* ***D.*** *Ifnγ mRNA* ***E.*** *Il-6 mRNA* ***F.*** *Stat1 mRNA* ***G.*** *Stat6 mRNA. All targets were normalized to Gapdh; mean (± SEM); n=5 per treatment group;, *p<0.05, **p<0.01, by two-way ANOVA and Šidák correction for multiple comparisons.*

IL-6, TNFα, IL-4, IFNγ) levels for many inflammatory markers following DE exposure (Cole *et al.,* 2016; Matta *et al.,* 2019). To corroborate these findings, and to test the hypothesis that these results would be exacerbated in the *Gclm*$^{+/-}$ mouse model, we analyzed cortex samples from DE-exposed mice for the presence of these markers via RT-qPCR (Fig. 3. 6). Comparable to previous studies with WT mice, DE-exposed *Gclm*$^{+/-}$ females saw an increase in *Il-1β* transcript levels (Fig. 3.6A, p=0.0053). Anti-inflammatory cytokine *Il-4* showed a trend to increase in DE-treated WT males only (Fig. 3.6B). Interestingly, *Gclm*$^{+/-}$ females did show an increase in *Tnfα* associated with developmental DE exposure which is potentially indicative of increased inflammation in the cortex that was amplified by GSH deficiency (Fig. 3.6C, p=0.0035). Transcription of the ASD-related cytokine *Ifnγ,* which is known to inhibit *Il-4* production, was found to increase in DE-treated *Gclm*$^{+/+}$ (WT) males (Fig. 3.6D, p=0.0141). These results were not exacerbated in *Gclm*$^{+/-}$ males, though *Gclm*$^{+/-}$ females did show a tendency to increase with DE exposure (Fig 3.6D). Unlike the previously found 12-fold and 8-fold increases in *Il-6* production found with acute DE exposure by Cole *et al.,* in microglial cells, this study showed no difference in exposure groups, although *Gclm*$^{+/+}$ males had significantly higher baseline *Il-6* expression (Fig. 3.6E, p=0.0095) (2016). Comparable to earlier studies described, dysregulated inflammatory mediation appeared to occur with DE exposure as measured by a decrease in *Stat1* levels in *Gclm*$^{+/+}$ mice of both sexes (Fig. 3.6F, p=0.0435). *Gclm*$^{+/-}$ males also saw a decrease with DE exposure (Fig. 3.6F, p=0.0191). *Stat6* showed no significant differences overall (Fig. 3.6E). These results were not supported in protein findings (Fig. 3.7), although we did observe a significant decrease in IFN-γ protein levels in DE exposed *Gclm*$^{+/-}$ females (Fig. 3.7A, p=0.0042).

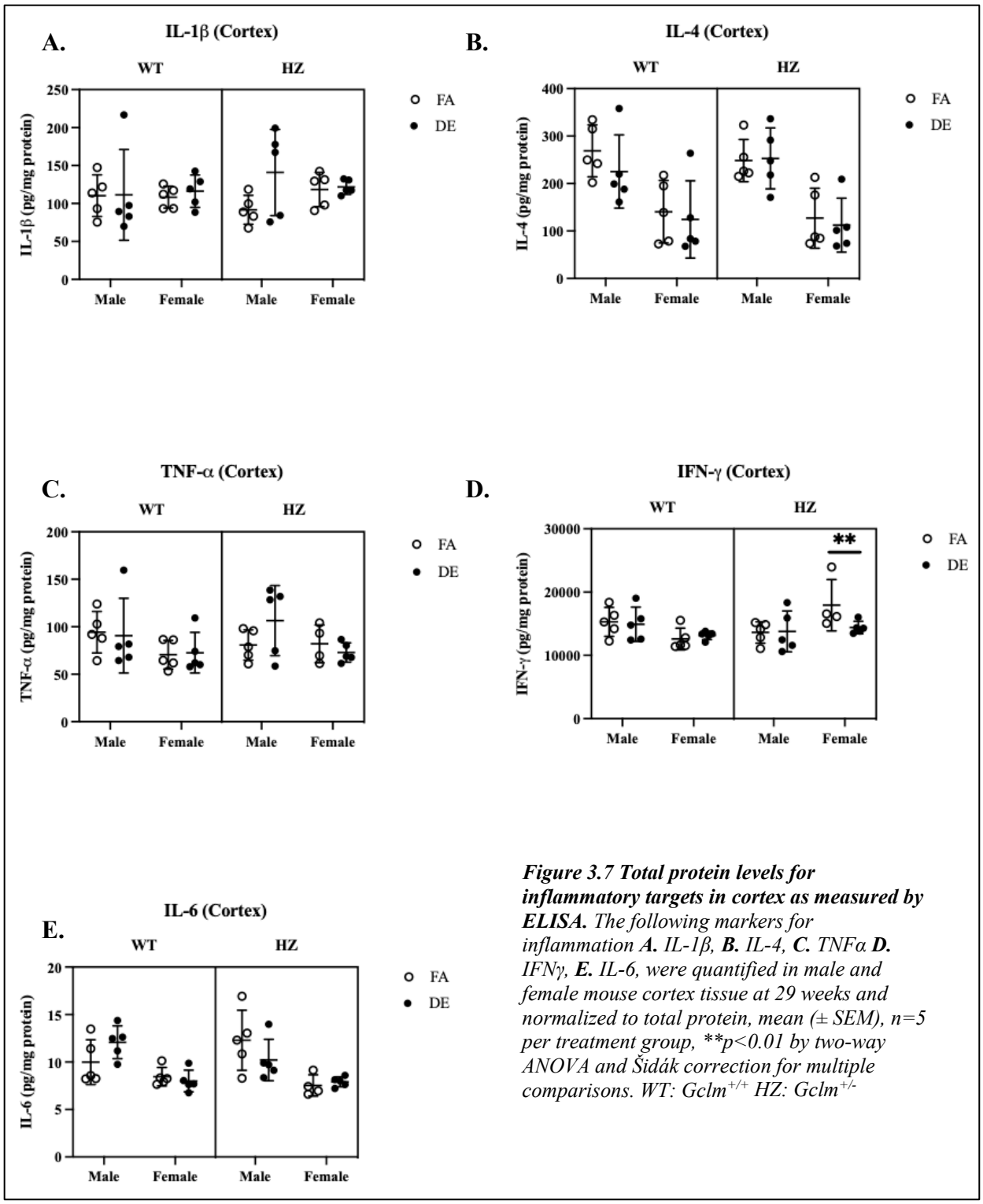

Figure 3.7 Total protein levels for inflammatory targets in cortex as measured by ELISA. *The following markers for inflammation* ***A.*** *IL-1β,* ***B.*** *IL-4,* ***C.*** *TNFα* ***D.*** *IFNγ,* ***E.*** *IL-6, were quantified in male and female mouse cortex tissue at 29 weeks and normalized to total protein, mean (± SEM), n=5 per treatment group, **p<0.01 by two-way ANOVA and Šidák correction for multiple comparisons. WT: Gclm$^{+/+}$ HZ: Gclm$^{+/-}$*

As TRAP in general is shown to cause oxidative stress in the brain, we measured lipid peroxidation in cortex samples from the DE- and FA-exposed mice. Lipid peroxidation is the

result of free radicals interacting with lipids, yielding oxidative damage *in vivo* and producing end-products such as MDA; therefore, levels of MDA were quantified via the TBARS assay as a measurement of oxidative stress levels in the brain. In previous studies, lipid peroxidation was shown to be increased in all brain regions following acute DE exposures of adult mice, and this effect was higher in males than in females (Cole *et al.,* 2016). In the current experiment, male and female mice of both genotypes showed a significant increase in MDA concentration following developmental exposure to DE, but males were not any more sensitive than females ($p<0.001$, $p<0.0001$ by Two-Way ANOVA), regardless of their genotype (Fig. 3.8). When comparing genotypes of the DE-exposed mice, $Gclm^{+/-}$ male mice had significantly higher MDA levels compared to $Gclm^{+/+}$ mice, supporting the idea that GSH was protective (Fig. 3.8).

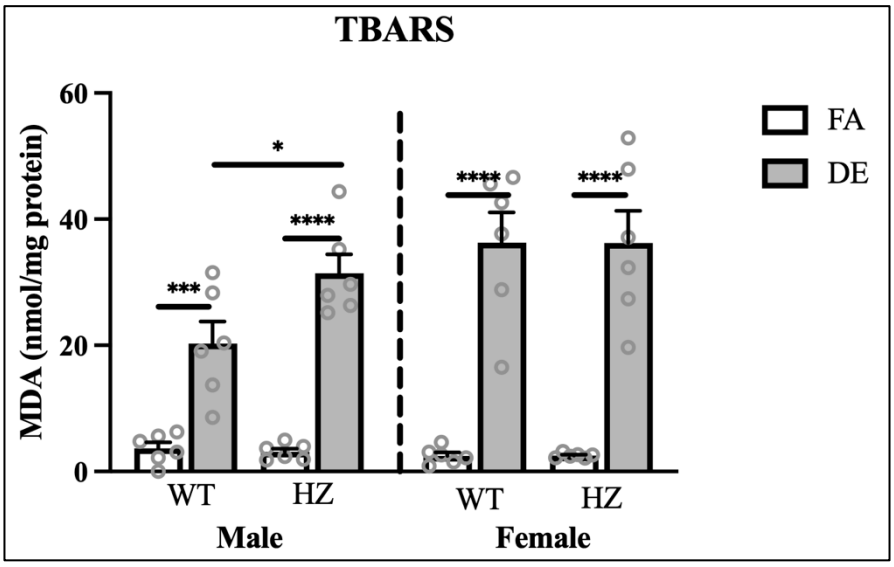

Figure 3.8 TBARS assay results in cortex tissue. *Measurement of lipid peroxidation via MDA concentration in male and female mice was normalized to total protein, N=6 per group, mean (± SEM), *p<0.05, **p<0.01, ***p<0.001, ****p<0.0001 by two-way ANOVA and Šidák correction for multiple comparisons. WT: $Gclm^{+/+}$ HZ: $Gclm^{+/-}$*

3.4 Microglial activation and neurodevelopment in the cortex of mice

Resident microglia have an important role in CNS maintenance; as innate immune cells they respond to numerous stimuli, including cellular damage and environmental stressors. Previously, acute exposure of adult mice to DE at 250-300 μg/m^3 revealed increased microglial activation along with amplified oxidative stress and neuroinflammation (Cole *et al.,* 2016; Costa *et al.,*

2016). Glial cells are seen as largely protective, but evidence has shown that chronic activation leads to release of pro-inflammatory mediators which can cause extreme neurotoxic effects (Muzio *et al.,* 2021). Because of its essential role in membrane ruffling, IBA1 was measured to quantify microglia activation in the cortex. As CD68 is indicative of phagocytic activity, it was measured as another marker for microglial activation. As had been found in previous studies (Bai *et al.,* 2019; Cheng *et al.,* 2016; Li *et al.,* 2021), male mice exposed developmentally to DE in the current study showed increased microglial activation in the cortex, as measured via IBA1 and CD68 RT-qPCR and/or Western blot. DE-exposed males showed an increase in transcript levels for *Iba1* (Fig. 3.9A, p=0.0298. Similarly, *Cd68* expression was increased in males exposed

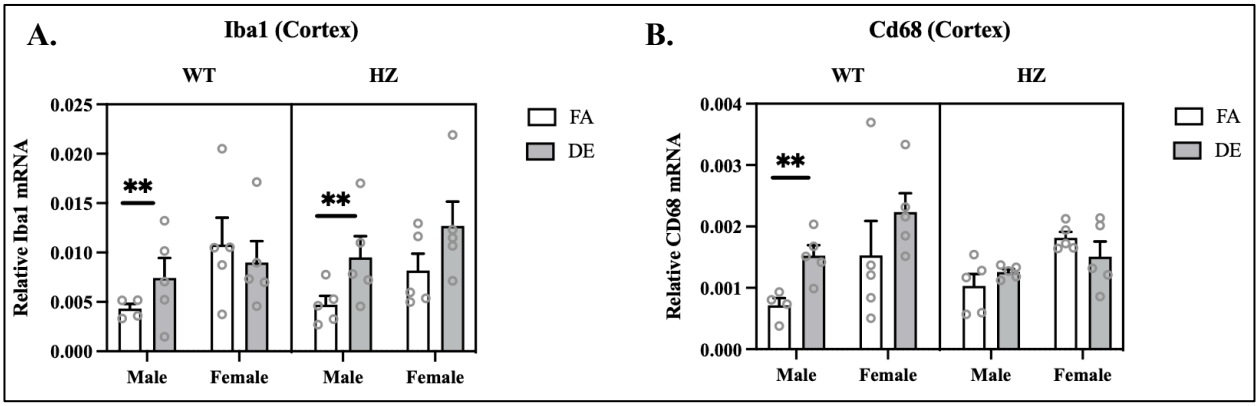

Figure 3.9 Transcript levels of microglial activation markers in mouse cortex tissue measured by qPCR. *Quantification of markers for microglial activation in male and female cortex tissue by qPCR* ***A.*** *Cd68 mRNA,* ***B.*** *Iba-1 mRNA targets normalized to GAPDH, mean (± SEM), n=5 per treatment group **p<0.01, by two-way ANOVA and Šidák correction for multiple comparisons.*

developmentally to DE (Fig. 3.9B, p=0.0036). In contrast to the previous studies of acute DE exposures in adult mice, the changes associated with developmental DE exposure were not exacerbated in *Gclm*$^{+/-}$ mice (Fig. 3.9). These results were not corroborated in protein analysis (Fig. 3.10A, B).

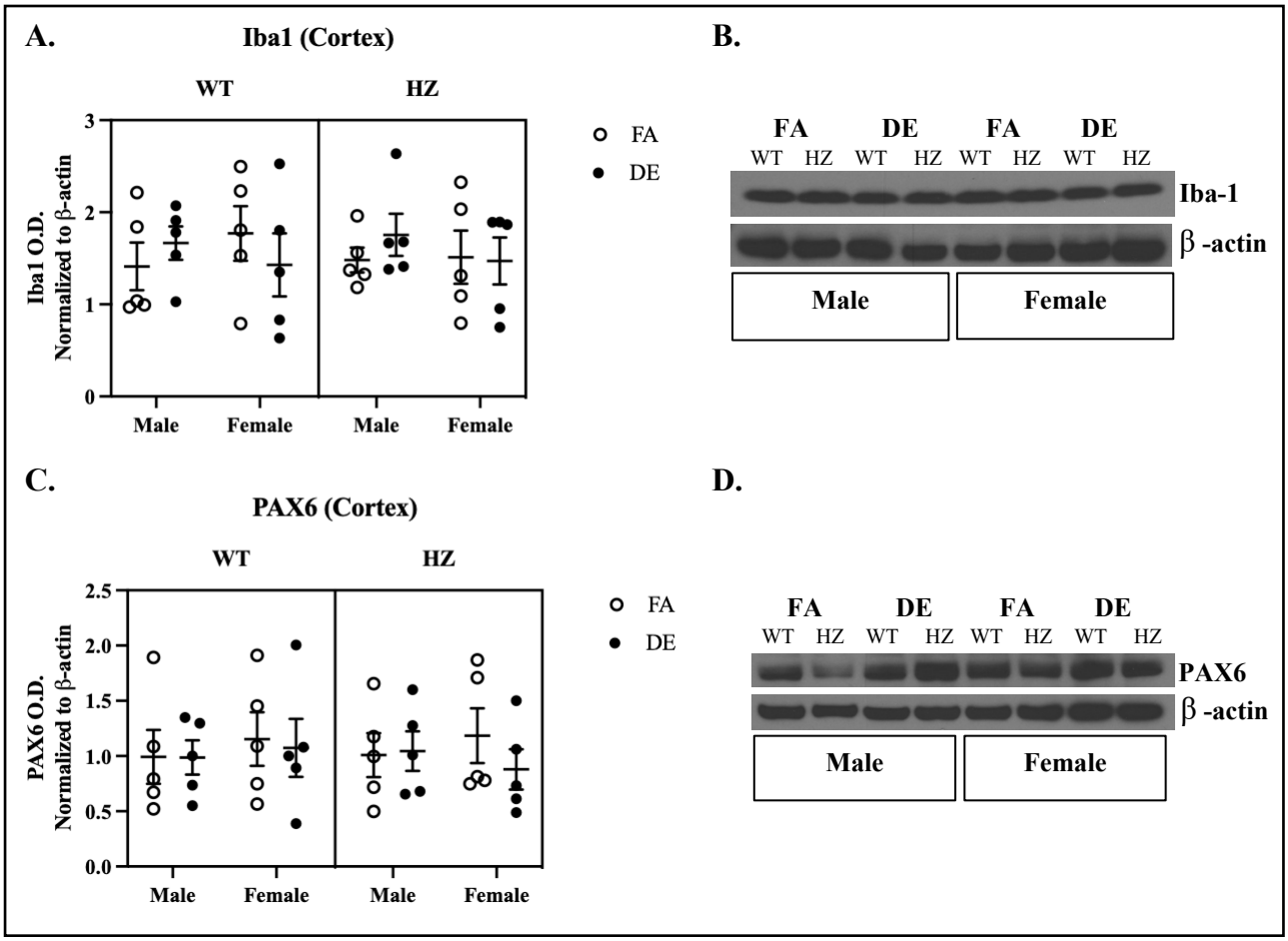

Figure 3.10 Microglial activation and neurotoxicity in mouse cortex tissue by Western blot analysis. A. *Microglial activation as measured in male and female mice by Iba1 levels in cortex, normalized to β-actin, mean (± SEM), n=5 per treatment group.* ***B.*** *Representative Western blot for IBA1.* ***C.*** *PAX6 levels measured in the cortex of male and female mice, normalized to β-actin, mean (± SEM), n=5 per treatment group.* ***D.*** *Representative Western blot for PAX6. All measures were not significant (ns) p>0.05 by two-way ANOVA and Šidák correction for multiple comparisons. WT: Gclm+/+ HZ: Gclm+/-*

Transcription factors have important roles during neurodevelopment. PAX6 has previously been found necessary for essential mechanisms involved in neurogenesis both *in vitro* and *in vivo* (Gan *et al.,* 2014; Sakurai & Osumi, 2008). Cole *et al*. also found upregulation of PAX6 in response to acute DE exposure in mice (2020). Dysregulated cortex development through increase of *Pax6* transcription was seen in DE treated mice as well (Chang *et al.,* 2018). Because interruption of corticogenesis has been linked to neurodevelopmental disorders, PAX6 is thought to be possibly involved in the pathogenesis of ASD (Kikkawa et al, 2019). In contrast to what was found by Chang *et al.,* DE treatment led to decreased *Pax6* transcript levels in males, and

this effect was the same in males of both genotypes (Fig. 3.11, p=0.0056). There was also a non-significant tendency towards decreased *Pax6* in DE-treated *Gclm*$^{+/-}$ females. In contrast, DE-treated *Gclm*$^{+/+}$ females tended to have an increase in *Pax6*, though this effect was not significant (Fig. 3.11). Neither effect was seen when measuring total protein levels (Fig. 3.10C, D).

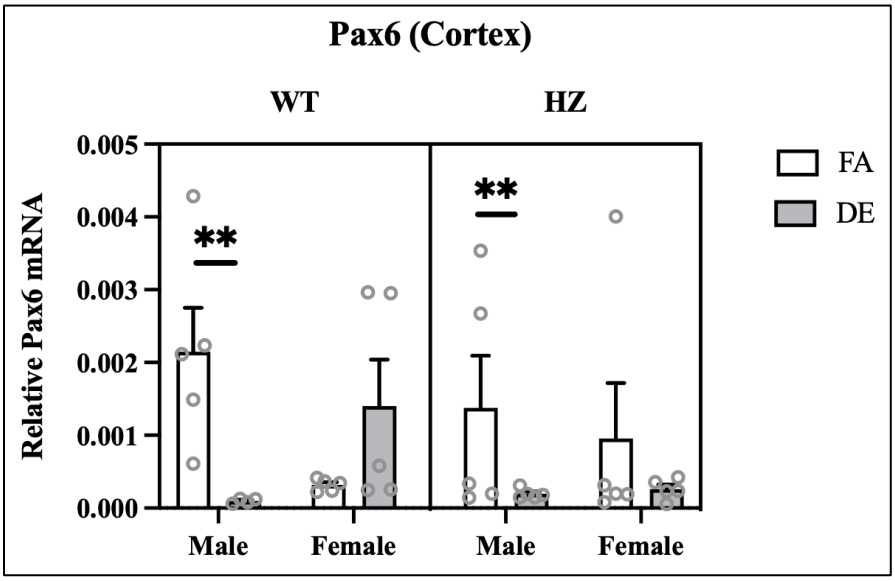

Figure 3.11 Transcript levels of ASD related marker PAX6 in mouse cortex tissue measured by qPCR. *Quantification of Pax6, ASD associated marker, mRNA in male and female cortex tissue by RT-qPCR. Targets normalized to GAPDH, mean (± SEM), n=5 per treatment group **p<0.01, by two-way ANOVA and Šidák correction for multiple comparisons.*

Discussion

Exposure to TRAP *in utero* and through childhood has been linked to an increased risk of developing ASD through both epidemiological studies (Calderón-Garcidueñas *et al.,* 2010; Chun *et al.,* 2020; Raz *et al.,* 2015; Roberts *et al.,* 2013; Volk *et al.,* 2011; 2013) and animal studies (Chang *et al.,* 2018; 2020; Cole *et al.,* 2020; Li *et al.,* 2018). Gene-environment interactions and temporal associations are difficult to determine in human epidemiological studies; thus, an *in vivo* exploration was conducted to gain insight on neurotoxic mechanisms associated with ASD etiology upon developmental exposure to DE. While this association has been connected consistently, gene-environment interactions as they relate to TRAP and CNS effects are poorly

understood. TRAP exposure has been associated with increased oxidative stress and neuroinflammation, and GSH is thought to be protective against these effects (Bai *et al.,* 2019; Cole *et al.,* 2016; Gu *et al.,* 2013; Nephew *et al.,* 2020; Weldy *et al.,* 2011). The findings of the current study indicate that perinatal exposure to DE is sufficient to induce neurotoxicity, as confirmed by increased repetitive behavior in the T-maze, decreased social behavior in the social preference test, as well as increased inflammation, oxidative stress, and microglial activation. However, the main hypothesis of the current study, that *Gclm*$^{+/-}$ mice would be more sensitive to the developmental neurotoxicity associated with DE exposure, was not supported by the findings. In several cases, the effects were remarkably the opposite of what was predicted – *Gclm*$^{+/-}$ mice were more resistant to the effects of DE exposure.

When considering behavior, previous results were largely substantiated in the current study. A significant decrease in spontaneous alternation was seen in DE exposed males, independent of genotype, suggesting that DE exposure is associated with increased repetitive behaviors. Spontaneous alternation tests exploratory behaviors as well as repetitive behaviors, which are controlled by many brain regions, including the hippocampus and the prefrontal cortex. Repetitive behaviors were also measured in the marble burying test, but no significant changes were found in DE-exposed mice.

Regarding inflammation and microglial activation, increased levels of *Ifnγ, Il-1β, Tnfα,* and *Cd68* were found in response to DE exposure, but these effects were not exacerbated in *Gclm*$^{+/-}$ mice. The resistance of *Gclm*$^{+/-}$ mice to neurodevelopmental toxicity of DE exposure could be explained by several factors, the most likely being a potential compensatory mechanism in

Gclm$^{+/-}$ mice similar to that reported in *Gclm* null (*Gclm*$^{-/-}$) mice (Weldy *et al.,* 2011). As *Gclm*$^{-/-}$ mice have increased antioxidant enzymes to protect from ROS, it is possible that the *Gclm*$^{+/-}$ mice develop a separate compensatory pathway when undergoing systemic inflammation; however, we should note that we still observed a significant increase in lipid peroxidation in the *Gclm*$^{+/-}$ mice compared to *Gclm*$^{+/+}$ mice. Since the induction of GCLC is the result of various upstream signaling pathways and its ability to synthesize GSH is not eliminated (only decreased by 10-15% in *Gclm*$^{+/-}$ mice), the NRF2 signaling pathway is a possible compensatory pathway of interest (Zhang & Forman, 2009). It is possible that there is a separate environmental variable enabling this NRF2 pathway, much like quercetin (a dietary flavonoid) was found to increase GSH activity through the pathway (Granado-Serrano *et al.,* 2012).

Another possible explanation for the appearance of a protective *Gclm*$^{+/-}$ mechanism is the increased baseline levels of *Il-6* present in WT mice, implying that some inflammatory targets had higher baseline levels in the cortex of *Gclm*$^{+/-}$ mice. The increased *Il-6* baseline could explain why we didn't see the typical increase in *Il-6* after DE exposures, therefore presenting *Gclm*$^{+/-}$ mice as less susceptible to the effects of DE in our study. Previous studies using a *Gclm* mouse model have shown that mRNA from two targets (*Il-6* and *Tnfα*) was not more highly elevated in *Gclm*$^{+/-}$ mice when compared to *Gclm null* mice; while the inflammatory cytokines at the protein level did show higher elevation in *Gclm*$^{+/-}$ mice (Weldy *et al.,* 2011). This could give some insight into discrepancies found in our study related to *Gclm*$^{+/-}$ susceptibility.

Expression of *Stat1* was decreased with DE treatment, though this was not confirmed across genotypes. Because increases of *Ifnγ* and various interleukins were observed following DE

exposure, we would expect *Stat1* TF to be upregulated as well, but this was not the case. This could be related to dysregulation of induced pluripotent stem cell development to NPC as seen in ASD. ELF3 is a key TF in neural induction, and STAT1 is a key TF in the cascade that activates ELF3; when compared to samples from typically developing participants the ELF3-STAT1 interaction was lost in ASD samples (Li *et al.,* 2012). Another ASD-associated TF we measured, *Pax6*, was found to decrease in the cortex of males following exposure to DE. PAX6 is highly related to ASD because of its role as a neurodevelopmental molecule that regulates brain development, neurogenesis, and gliogenesis (Kikkawa wt al., 2019). Behavioral deficiencies in rodent models with decreased PAX6 function have been observed (Tuoc *et al.,* 2009; Umeda *et al.,* 2010; Yoshizaki *et al.,* 2016).

Interestingly, in our study, the transcript levels did not predict protein levels. This is fascinating, as correlating mRNA and protein measurements in complex samples is a disputed act in the field of proteomics, especially with more precise methods developing constantly. This debate could rationalize why the protein levels did not confirm many of the RT-qPCR findings. A study based on RNA-binding found these discrepancies in healthy tissue and through computational analysis found several translational regulators that could be responsible for these discrepancies (Wu *et al.,* 2020). There are many steps in the processes involved in translation of mRNA to protein that could be leading to this, including potential proteolysis occurring during transcription leading to decreased protein level changes but increased transcription level changes.

Though some of the findings from previous studies in our lab (Chang *et al.,* 2018, 2020; Cole *et al.,* 2016, 2020) were not confirmed by our findings, and our hypothesis that *Gclm*$^{+/-}$ mice would

be more sensitive to the effects of developmental DE exposure was not supported, the current study clearly showed that developmental DE exposure was associated with increases in oxidative stress, neuroinflammation and ASD-related behaviors. Many of our findings were also sex specific, with males, in general, seeing a greater effect when exposed to DE, which has relevance considering that a higher incidence of ASD is seen in people assigned male at birth (Rice *et al.,* 2012). The relative resistance of *Gclm*$^{+/-}$ mice to these neurotoxic effects was surprising, given the previously seen sensitivity of these mice to acute DE effects in adulthood and the importance of GSH for protection against oxidative stress. More investigation is necessary to explore this effect further. At least some of the variance in findings could be due to clear study differences between Chang et al. and what was implemented for these experiments. The obvious difference was that in the previous study behavioral assessments were conducted at 6-weeks (PND42), 7-weeks (PND49), and 8-weeks (PND56); while biochemical endpoints were conducted on mice at PND3, PND21, and PND60 (Chang *et al.,* 2018, 2019). As previously mentioned, due to the COVID-19 public health emergency our testing schedule was pushed back significantly. For this study, behavioral tests were conducted on the following timeline—T-maze at 12 weeks (PND72), social preference at 24 weeks (PND144), and marble burying at 26 weeks (PND182), while all biochemical endpoints were tested on 29-week samples (PND203). There was a surprising persistence in oxidative stress, which has not been seen in other published studies. This difference in findings paired with the fact that oxidative stress was the only effect that was clearly increased in *Gclm*$^{+/-}$ mice could be a positive finding, showing that prenatal exposures to AP may not be as pathogenically impactful as previously thought after a substantial recovery period following ceasing exposures. This difference could also allude to a potential reversibility

of neurodevelopmental impacts since many of the findings from the previous studies were not found to persist at these later ages.

Finally, it's worth noting that the strain background of the exposed dams in the current study was C57Bl/6, whereas the *Gclm*$^{+/-}$ sires were derived from a genetically-distinct *Gclm* background strain that had been backcrossed to C57Bl/6 mice for 6 generations. In contrast, both the dams and sires in the previous studies (Chang *et al.,* 2018, 2019) were WT mice of the same C57Bl/6 background strain. Thus, the pups in the current study would be of slightly different genetic background than in the previous studies. There is a likelihood that this could have led to small genetic differences. It is also possible that the dam's genetic susceptibility during exposure has more impact than previously presumed, in which case the offspring of *Gclm*$^{+/-}$ dams might be more susceptible than those of the C57Bl/6J dams. If the dam is potentially creating a GSH rich environment where oxidative stress has a more difficult time thriving, then it is possible that *in utero* the pup is protected from exposure during these important neurodevelopmental stages. This could be explained by evidence supporting the effects of maternal immune activation on neurodevelopmental outcomes, like ASD (Estes & McAllister, 2016).

Conclusion

Current findings from this study provide additional evidence that developmental DE exposure causes adverse CNS effects and indicate that some of these effects can persist as late as 29 weeks post-exposure. DE-exposed mice exhibited increased lipid peroxidation, altered expression of inflammatory cytokines, and alterations in some ASD-related behaviors. Surprisingly, the findings of this study do not support our hypothesis that *Gclm*$^{+/-}$ mice would be more susceptible

to these effects. Indeed, in some cases, *Gclm*$^{+/-}$ mice had opposite effects to what was predicted, showing resistance to many of the adverse CNS effects following developmental DE exposure. The exception is lipid peroxidation, which was higher in the cortex of *Gclm*$^{+/-}$ males than *Gclm*$^{+/+}$ males following DE exposure. The modification of the timeline for biochemical endpoint measurements (~20-week difference from previous studies) should also be emphasized, because of our diminished findings this difference could be considered a possible "recovery period" which is still valued knowledge. Overall, these findings add to the growing evidence of the negative impact that AP has on health outcomes though there is probable indication that some of these impacts could potentially be reversible or, in some measure, not maintain permanence through adulthood.

Future Directions

Further evidence is needed regarding gene-environment interactions as a critical factor in the susceptibility to ASD. Possibly a much larger study with multiple exposure mixtures to account for the distinctive profile of AP. There is evidence to suggest that adverse health effects could also be related to elements generated from road wear, brake-pads, and vehicle machinery, and that these have become more important with the progressive reductions in exhaust emissions. Future studies could concentrate on effects from these less studied AP contributors (Han & Naeher, 2006). Although previous studies utilizing dams of *Gclm*$^{+/-}$ background yielded poor birth outcomes it would be beneficial to address genetic differences in the dams during a perinatal exposure.

More evidence is needed to establish temporality as it relates to the development of ASD as well as direct neurotoxic mechanisms. It would be worthwhile to follow an experimental timeline more like that of the previous studies (Chang *et al.,* 2018, 2019), without a recovery period between exposures and testing, while again testing genetic susceptibility through use of the *Gclm* model. Though direct causality is yet to be established, it is becoming more apparent that neurodevelopmental effects of AP exposure are less related to a specific mechanism or disease. It is more likely the result of many changes that result in a biological environment that impairs proper CNS development.

References

Aoki, Y., Abe, O., Nippashi, Y., & Yamasue, H. (2013). Comparison of white matter integrity between autism spectrum disorder subjects and typically developing individuals: A meta-analysis of diffusion tensor imaging tractography studies. *Molecular Autism*, *4*, 25. https://doi.org/10.1186/2040-2392-4-25

Bai, K.-J., Chuang, K.-J., Chen, C.-L., Jhan, M.-K., Hsiao, T.-C., Cheng, T.-J., Chang, L.-T., Chang, T.-Y., & Chuang, H.-C. (2019). Microglial activation and inflammation caused by traffic-related particulate matter. *Chemico-Biological Interactions*, *311*, 108762. https://doi.org/10.1016/j.cbi.2019.108762

Bandyopadhyay, A. (2016). Neurological Disorders from Ambient (Urban) Air Pollution Emphasizing UFPM and PM2.5. *Current Pollution Reports*, *2*(3), 203–211. https://doi.org/10.1007/s40726-016-0039-z

Block, M. L., & Calderón-Garcidueñas, L. (2009). Air pollution: Mechanisms of neuroinflammation and CNS disease. *Trends in Neurosciences*, *32*(9), 506–516. https://doi.org/10.1016/j.tins.2009.05.009

Botta, D., White, C. C., Vliet-Gregg, P., Mohar, I., Shi, S., McGrath, M. B., McConnachie, L. A., & Kavanagh, T. J. (2008). Modulating GSH Synthesis Using Glutamate Cysteine Ligase Transgenic and Gene-Targeted Mice. *Drug Metabolism Reviews*, *40*(3), 465–477. https://doi.org/10.1080/03602530802186587

Bourdrel, T., Bind, M.-A., Béjot, Y., Morel, O., & Argacha, J.-F. (2017). Cardiovascular effects of air pollution. *Archives of Cardiovascular Diseases*, *110*(11), 634–642. https://doi.org/10.1016/j.acvd.2017.05.003

Brook, R. D., Rajagopalan, S., Pope, C. A., Brook, J. R., Bhatnagar, A., Diez-Roux, A. V., Holguin, F., Hong, Y., Luepker, R. V., Mittleman, M. A., Peters, A., Siscovick, D., Smith, S. C., Whitsel, L., & Kaufman, J. D. (2010). Particulate Matter Air Pollution and Cardiovascular Disease. *Circulation*, *121*(21), 2331–2378. https://doi.org/10.1161/CIR.0b013e3181dbece1

Calderón-Garcidueñas, L., Azzarelli, B., Acuna, H., Garcia, R., Gambling, T. M., Osnaya, N., Monroy, S., Del Rosario Tizapantzi, M., Carson, J. L., Villarreal-Calderon, A., & Rewcastle, B. (2002). Air Pollution and Brain Damage. *Toxicologic Pathology*, *30*(3), 373–389. https://doi.org/10.1080/01926230252929954

Calderón-Garcidueñas, L., Franco-Lira, M., Henríquez-Roldán, C., Osnaya, N., González-Maciel, A., Reynoso-Robles, R., Villarreal-Calderon, R., Herritt, L., Brooks, D., Keefe, S., Palacios-Moreno, J., Villarreal-Calderon, R., Torres-Jardón, R., Medina-Cortina, H., Delgado-Chávez, R., Aiello-Mora, M., Maronpot, R. R., & Doty, R. L. (2010). Urban air pollution: Influences on olfactory function and pathology in exposed children and young adults. *Experimental and Toxicologic Pathology*, *62*(1), 91–102. https://doi.org/10.1016/j.etp.2009.02.117

Calderón-Garcidueñas, L., Leray, E., Heydarpour, P., Torres-Jardón, R., & Reis, J. (2016). Air pollution, a rising environmental risk factor for cognition, neuroinflammation and neurodegeneration: The clinical impact on children and beyond. *Revue Neurologique*, *172*(1), 69–80. https://doi.org/10.1016/j.neurol.2015.10.008

Chang, Y.-C., Cole, T. B., & Costa, L. G. (2017). Behavioral Phenotyping for Autism Spectrum Disorders in Mice. *Current Protocols in Toxicology*, *72*, 11.22.1-11.22.21. https://doi.org/10.1002/cptx.19

Chang, Y.-C., Cole, T. B., & Costa, L. G. (2018). Prenatal and early-life diesel exhaust exposure causes autism-like behavioral changes in mice. *Particle and Fibre Toxicology*, *15*(1). https://doi.org/10.1186/s12989-018-0254-4

Chang, Y.-C., Daza, R., Hevner, R., Costa, L. G., & Cole, T. B. (2019). Prenatal and early life diesel exhaust exposure disrupts cortical lamina organization: Evidence for a reelin-related pathogenic pathway induced by interleukin-6. *Brain, Behavior, and Immunity*, *78*, 105–115. https://doi.org/10.1016/j.bbi.2019.01.013

Chen, J.-C., & Schwartz, J. (2009). Neurobehavioral effects of ambient air pollution on cognitive performance in US adults. *Neurotoxicology*, *30*(2), 231–239. https://doi.org/10.1016/j.neuro.2008.12.011

Cheng, H., Saffari, A., Sioutas, C., Forman, H. J., Morgan, T. E., & Finch, C. E. (2016). Nanoscale Particulate Matter from Urban Traffic Rapidly Induces Oxidative Stress and Inflammation in Olfactory Epithelium with Concomitant Effects on Brain. *Environmental Health Perspectives*, *124*(10), 1537–1546. https://doi.org/10.1289/EHP134

Chiu, Y.-H. M., Bellinger, D. C., Coull, B. A., Anderson, S., Barber, R., Wright, R. O., & Wright, R. J. (2013). Associations between Traffic-Related Black Carbon Exposure and Attention in a Prospective Birth Cohort of Urban Children. *Environmental Health Perspectives*, *121*(7), 859–864. https://doi.org/10.1289/ehp.1205940

Chun, H., Leung, C., Wen, S. W., McDonald, J., & Shin, H. H. (2020). Maternal exposure to air pollution and risk of autism in children: A systematic review and meta-analysis. *Environmental Pollution*, *256*, 113307. https://doi.org/10.1016/j.envpol.2019.113307

Cole, T. B., Chang, Y.-C., Dao, K., Daza, R., Hevner, R., & Costa, L. G. (2020). Developmental exposure to diesel exhaust upregulates transcription factor expression, decreases hippocampal neurogenesis, and alters cortical lamina organization: Relevance to neurodevelopmental disorders. *Journal of Neurodevelopmental Disorders*, *12*, 41. https://doi.org/10.1186/s11689-020-09340-3

Cole, T. B., Coburn, J., Dao, K., Roqué, P., Chang, Y.-C., Kalia, V., Guilarte, T. R., Dziedzic, J., & Costa, L. G. (2016). Sex and genetic differences in the effects of acute diesel exhaust exposure on inflammation and oxidative stress in mouse brain. *Toxicology*, *374*, 1–9. https://doi.org/10.1016/j.tox.2016.11.010

Cole, T. B., Giordano, G., Co, A. L., Mohar, I., Kavanagh, T. J., & Costa, L. G. (2011). Behavioral Characterization of GCLM-Knockout Mice, a Model for Enhanced Susceptibility to Oxidative Stress. *Journal of Toxicology*, *2011*. https://www.proquest.com/docview/868073872/abstract/A308841FD9F24F83PQ/1

Cory-Slechta, D. A., Sobolewski, M., Marvin, E., Conrad, K., Merrill, A., Anderson, T., Jackson, B. P., & Oberdorster, G. (2019). The Impact of Inhaled Ambient Ultrafine Particulate Matter on Developing Brain: Potential Importance of Elemental Contaminants. *Toxicologic Pathology*, *47*(8), 976–992. https://doi.org/10.1177/0192623319878400

Costa, L. G., Chang, Y.-C., & Cole, T. B. (2017). Developmental Neurotoxicity of Traffic-Related Air Pollution: Focus on Autism. *Current Environmental Health Reports*, *4*(2), 156–165. https://doi.org/10.1007/s40572-017-0135-2

Costa, L. G., Cole, T. B., Coburn, J., Chang, Y.-C., Dao, K., & Roque, P. (2014a). Neurotoxicants are in the air: Convergence of human, animal, and in vitro studies on the effects of air pollution on the brain. *BioMed Research International*. https://doi.org/ 10.1155/2014/736385

Costa, L. G., Cole, T. B., Dao, K., Chang, Y.-C., Coburn, J., & Garrick, J. (2019). Chapter Seven - Neurotoxicity of air pollution: Role of neuroinflammation. In M. Aschner & L. G. Costa (Eds.), *Advances in Neurotoxicology* (Vol. 3, pp. 195–221). Academic Press. https://doi.org/10.1016/bs.ant.2018.10.007

Costa, L. G., Cole, T. B., Dao, K., Chang, Y.-C., Coburn, J., & Garrick, J. M. (2020). Effects of air pollution on the nervous system and its possible role in neurodevelopmental and neurodegenerative disorders. *Pharmacology & Therapeutics*, *210*, 107523. https://doi.org/10.1016/j.pharmthera.2020.107523

Costa, L. G., Cole, T. B., Dao, K., Chang, Y.-C., & Garrick, J. M. (2019). Developmental impact of air pollution on brain function. *Neurochemistry International*, *131*, 104580. https://doi.org/10.1016/j.neuint.2019.104580

Costa, L. G., Fattori, V., Giordano, G., & Vitalone, A. (2007). An in vitro approach to assess the toxicity of certain food contaminants: Methylmercury and polychlorinated biphenyls. *Toxicology*, *237*(1), 65–76. https://doi.org/10.1016/j.tox.2007.05.003

Costa, L. G., Garrick, J. M., Dao, K., Phillips, A., Marsillach, J., & Cole, T. B. (2022). Chapter 42—Traffic-related air pollution and the developing brain. In R. C. Gupta (Ed.), *Reproductive and Developmental Toxicology (Third Edition)* (pp. 833–843). Academic Press. https://doi.org/10.1016/B978-0-323-89773-0.00042-4

Costa, L. G., Garrick, J. M., Roque, P. J., & Pellacani, C. (2016). Mechanisms of Neuroprotection by Quercetin: Counteracting Oxidative Stress and More. *Oxidative Medicine and Cellular Longevity*, *2016*. https://doi.org/10.1155/2016/2986796

Costa, L. G., Tait, L., de Laat, R., Dao, K., Giordano, G., Pellacani, C., Cole, T. B., & Furlong, C. E. (2014b). Modulation of paraoxonase 2 (PON2) in mouse brain by the polyphenol quercetin: A mechanism of neuroprotection? *Neurochemical Research*, *38*(9), 1809–1818. https://doi.org/10.1007/s11064-013-1085-1

Davoli-Ferreira, M., Thomson, C. A., & McCoy, K. D. (2021). Microbiota and Microglia Interactions in ASD. *Frontiers in Immunology*, *12*. https://www.frontiersin.org/article/10.3389/fimmu.2021.676255

Dutheil, F., Comptour, A., Morlon, R., Mermillod, M., Pereira, B., Baker, J. S., Charkhabi, M., Clinchamps, M., & Bourdel, N. (2021). Autism spectrum disorder and air pollution: A systematic review and meta-analysis. *Environmental Pollution*, *278*, 116856. https://doi.org/10.1016/j.envpol.2021.116856

Estes, M. L., & McAllister, A. K. (2016). Maternal immune activation: Implications for neuropsychiatric disorders. *Science*, *353*(6301), 772–777. https://doi.org/10.1126/science.aag3194

Flores-Pajot, M.-C., Ofner, M., Do, M. T., Lavigne, E., & Villeneuve, P. J. (2016). Childhood autism spectrum disorders and exposure to nitrogen dioxide, and particulate matter air pollution: A review and meta-analysis. *Environmental Research*, *151*, 763–776. https://doi.org/10.1016/j.envres.2016.07.030

Fox, J. R., Cox, D. P., Drury, B. E., Gould, T. R., Kavanagh, T. J., Paulsen, M. H., Sheppard, L., Simpson, C. D., Stewart, J. A., Larson, T. V., & Kaufman, J. D. (2015). Chemical characterization and in vitro toxicity of diesel exhaust particulate matter generated under varying conditions. *Air Quality, Atmosphere, & Health*, *8*(5), 507–519. https://doi.org/10.1007/s11869-014-0301-8

Franklin, C. C., Backos, D. S., Mohar, I., White, C. C., Forman, H. J., & Kavanagh, T. J. (2009). Structure, function, and post-translational regulation of the catalytic and modifier subunits of glutamate cysteine ligase. *Molecular Aspects of Medicine*, *30*(1–2), 86–98. https://doi.org/10.1016/j.mam.2008.08.009

Gan, Q., Lee, A., Suzuki, R., Yamagami, T., Stokes, A., Nguyen, B. C., Pleasure, D., Wang, J., Chen, H., & Zhou, C. J. (2014). Pax6 Mediates β-Catenin Signaling for Self-Renewal and Neurogenesis by Neocortical Radial Glial Stem Cells. *Stem Cells (Dayton, Ohio)*, *32*(1), 45–58. https://doi.org/10.1002/stem.1561

Garrick, J. M., Dao, K., de Laat, R., Elsworth, J., Cole, T. B., Marsillach, J., Furlong, C. E., & Costa, L. G. (2016). Developmental expression of paraoxonase 2. *Chemico-Biological Interactions*, *259*, 168–174. https://doi.org/10.1016/j.cbi.2016.04.001

Gill, E. A., Curl, C. L., Adar, S. D., Allen, R. W., Auchincloss, A. H., O'Neill, M. S., Park, S. K., Van Hee, V. C., Diez Roux, A. V., & Kaufman, J. D. (2011). Air Pollution and Cardiovascular Disease in the Multi-Ethnic Study of Atherosclerosis. *Progress in Cardiovascular Diseases*, *53*(5), 353–360. https://doi.org/10.1016/j.pcad.2011.02.001

Giordano, G., Afsharinejad, Z., Guizzetti, M., Vitalone, A., Kavanagh, T. J., & Costa, L. G. (2007). Organophosphorus insecticides chlorpyrifos and diazinon and oxidative stress in neuronal cells in a genetic model of glutathione deficiency. *Toxicology and Applied Pharmacology*, *219*(2), 181–189. https://doi.org/10.1016/j.taap.2006.09.016

Giordano, G., White, C. C., McConnachie, L. A., Fernandez, C., Kavanagh, T. J., & Costa, L. G. (2006). Neurotoxicity of Domoic Acid in Cerebellar Granule Neurons in a Genetic Model of Glutathione Deficiency. *Molecular Pharmacology*, *70*(6), 2116–2126. https://doi.org/10.1124/mol.106.027748

Global Burden of Disease Collaborative Network. Global Burden of Disease Study 2019 (GBD 2019) Reference Life Table. Seattle, United States of America: Institute for Health Metrics and Evaluation (IHME), 2021. https://doi.org/10.6069/1D4Y-YQ37

Gould, T., Larson, T., Stewart, J., Kaufman, J. D., Slater, D., & McEwen, N. (2008). A Controlled Inhalation Diesel Exhaust Exposure Facility with Dynamic Feedback Control of PM Concentration. *Inhalation Toxicology*, *20*(1), 49–52. https://doi.org/10.1080/08958370701758478

Granado-Serrano, A. B., Martín, M. A., Bravo, L., Goya, L., & Ramos, S. (2012). Quercetin modulates Nrf2 and glutathione-related defenses in HepG2 cells: Involvement of p38. *Chemico-Biological Interactions*, *195*(2), 154–164. https://doi.org/10.1016/j.cbi.2011.12.005

Greenbaum, D. S. (2013). CHAPTER 5. SOURCES OF AIR POLLUTION: GASOLINE AND DIESEL ENGINES. In K. Straif, A. Cohen, & J. M. Samet (Eds.), *Air Pollution and Cancer*. https://publications.iarc.fr/Book-And-Report-Series/Iarc-Scientific-Publications/Air-Pollution-And-Cancer-2013

Gu, F., Chauhan, V., & Chauhan, A. (2013). Impaired synthesis and antioxidant defense of glutathione in the cerebellum of autistic subjects: Alterations in the activities and protein expression of glutathione-related enzymes. *Free Radical Biology and Medicine*, *65*, 488–496. https://doi.org/10.1016/j.freeradbiomed.2013.07.021

Guxens, M., Garcia-Esteban, R., Giorgis-Allemand, L., Forns, J., Badaloni, C., Ballester, F., Beelen, R., Cesaroni, G., Chatzi, L., de Agostini, M., de Nazelle, A., Eeftens, M., Fernandez, M. F., Fernández-Somoano, A., Forastiere, F., Gehring, U., Ghassabian, A., Heude, B., Jaddoe, V. W. V., … Sunyer, J. (2014). Air Pollution During Pregnancy and Childhood Cognitive and Psychomotor Development: Six European Birth Cohorts. *Epidemiology*, *25*(5), 636–647. https://doi.org/10.1097/EDE.0000000000000133

Hankey, S., Marshall, J. D., & Brauer, M. (2012). Health Impacts of the Built Environment: Within-Urban Variability in Physical Inactivity, Air Pollution, and Ischemic Heart Disease Mortality. *Environmental Health Perspectives*, *120*(2), 247–253. https://doi.org/10.1289/ehp.1103806

Institute for Laboratory Animal Research (U.S.), National Academies Press (U.S.), & National Research Council (U.S.). Committee for the Update of the Guide for the Care and Use of Laboratory Animals. $$Q National Research Council U.S. . Committee for the Update of the Guide for the Care and Use of Laboratory Animals. (2011). *Guide for the care and use of laboratory animals* (8th ed.). Washington, D.C. : National Academies Press.

Jankowska-Kieltyka, M., Roman, A., & Nalepa, I. (2021). The Air We Breathe: Air Pollution as a Prevalent Proinflammatory Stimulus Contributing to Neurodegeneration. *Frontiers in Cellular Neuroscience*, *15*. https://www.frontiersin.org/article/10.3389/fncel.2021.647643

Jung, C.-R., Lin, Y.-T., & Hwang, B.-F. (2013). Air Pollution and Newly Diagnostic Autism Spectrum Disorders: A Population-Based Cohort Study in Taiwan. *PLOS ONE*, *8*(9), e75510. https://doi.org/10.1371/journal.pone.0075510

Kaplan, M. H. (2013). STAT signaling in inflammation. *JAK-STAT*, *2*(1), e24198. https://doi.org/10.4161/jkst.24198

Kierdorf, K., & Prinz, M. (2013). Factors regulating microglia activation. *Frontiers in Cellular Neuroscience*, *7*. https://www.frontiersin.org/article/10.3389/fncel.2013.00044

Kikkawa, T., Casingal, C. R., Chun, S. H., Shinohara, H., Hiraoka, K., & Osumi, N. (2019). The role of Pax6 in brain development and its impact on pathogenesis of autism spectrum disorder. *Brain Research*, *1705*, 95–103. https://doi.org/10.1016/j.brainres.2018.02.041

Kilian, J., & Kitazawa, M. (2018). The emerging risk of exposure to air pollution on cognitive decline and Alzheimer's disease – Evidence from epidemiological and animal studies. *Biomedical Journal*, *41*(3), 141–162. https://doi.org/10.1016/j.bj.2018.06.001

Kraft, A. D., & Harry, G. J. (2011). Features of Microglia and Neuroinflammation Relevant to Environmental Exposure and Neurotoxicity. *International Journal of Environmental Research and Public Health*, *8*(7), 2980–3018. https://doi.org/10.3390/ijerph8072980

Kumar, P., Morawska, L., Birmili, W., Paasonen, P., Hu, M., Kulmala, M., Harrison, R. M., Norford, L., & Britter, R. (2014). Ultrafine particles in cities. *Environment International*, *66*, 1–10. https://doi.org/10.1016/j.envint.2014.01.013

Lepeule, J., Laden, F., Dockery, D., & Schwartz, J. (2012). Chronic Exposure to Fine Particles and Mortality: An Extended Follow-up of the Harvard Six Cities Study from 1974 to 2009. *Environmental Health Perspectives*, *120*(7), 965–970. https://doi.org/10.1289/ehp.1104660

Levesque, S., Surace, M. J., McDonald, J., & Block, M. L. (2011). Air pollution & the brain: Subchronic diesel exhaust exposure causes neuroinflammation and elevates early markers of neurodegenerative disease. *Journal of Neuroinflammation*, *8*(1), 105. https://doi.org/10.1186/1742-2094-8-105

Li, D., Xu, J., & Yang, M. Q. (2021). Gene Regulation Analysis Reveals Perturbations of Autism Spectrum Disorder during Neural System Development. *Genes*, *12*(12), 1901. https://doi.org/10.3390/genes12121901

Long, E., Schwartz, C., & Carlsten, C. (2022). Controlled human exposure to diesel exhaust: A method for understanding health effects of traffic-related air pollution. *Particle and Fibre Toxicology*, *19*(1), 15. https://doi.org/10.1186/s12989-022-00454-1

Maheswaran, R. (2016). Air pollution and stroke – an overview of the evidence base. *Spatial and Spatio-Temporal Epidemiology*, *18*, 74–81. https://doi.org/10.1016/j.sste.2016.04.004

Masi, A., Quintana, D. S., Glozier, N., Lloyd, A. R., Hickie, I. B., & Guastella, A. J. (2015). Cytokine aberrations in autism spectrum disorder: A systematic review and meta-analysis. *Molecular Psychiatry*, *20*(4), 440–446. https://doi.org/10.1038/mp.2014.59

Matta, S. M., Hill-Yardin, E. L., & Crack, P. J. (2019). The influence of neuroinflammation in Autism Spectrum Disorder. *Brain, Behavior, and Immunity*, *79*, 75–90. https://doi.org/10.1016/j.bbi.2019.04.037

McConnachie, L. A., Mohar, I., Hudson, F. N., Ware, C. B., Ladiges, W. C., Fernandez, C., Chatterton-Kirchmeier, S., White, C. C., Pierce, R. H., & Kavanagh, T. J. (2007). Glutamate Cysteine Ligase Modifier Subunit Deficiency and Gender as Determinants of Acetaminophen-Induced Hepatotoxicity in Mice. *Toxicological Sciences*, *99*(2), 628–636. https://doi.org/10.1093/toxsci/kfm165

McGuinn, L. A., Wiggins, L. D., Volk, H. E., Qian, D., Moody, E. J., Kasten, E., Link to external site, this link will open in a new window, Schwartz, J., Wright, R. O., Schieve, L. A., Windham, G. C., Link to external site, this link will open in a new window, & Daniels, J. L. (2022). Pre- and Postnatal Fine Particulate Matter Exposure and Childhood Cognitive and Adaptive Function. *International Journal of Environmental Research and Public Health*, *19*(7), 3748. https://doi.org/10.3390/ijerph19073748

Mookherjee, N., Ryu, M. H., Hemshekhar, M., Orach, J., Spicer, V., & Carlsten, C. (2022). Defining the effects of traffic-related air pollution on the human plasma proteome using an aptamer proteomic array: A dose-dependent increase in atherosclerosis-related proteins. *Environmental Research*, *209*, 112803. https://doi.org/10.1016/j.envres.2022.112803

Morris-Schaffer, K., Merrill, A., Jew, K., Wong, C., Conrad, K., Harvey, K., Marvin, E., Sobolewski, M., Oberdörster, G., Elder, A., & Cory-Slechta, D. A. (2019a). Effects of neonatal inhalation exposure to ultrafine carbon particles on pathology and behavioral outcomes in C57BL/6J mice. *Particle and Fibre Toxicology*, *16*(1), 10. https://doi.org/10.1186/s12989-019-0293-5

Morris-Schaffer, K., Merrill, A. K., Wong, C., Jew, K., Sobolewski, M., & Cory-Slechta, D. A. (2019b). Limited developmental neurotoxicity from neonatal inhalation exposure to diesel exhaust particles in C57BL/6 mice. *Particle and Fibre Toxicology*, *16*, 1. https://doi.org/10.1186/s12989-018-0287-8

Murray, C. J. L., Aravkin, A. Y., Zheng, P., Abbafati, C., Abbas, K. M., Abbasi-Kangevari, M., Abd-Allah, F., Abdelalim, A., Abdollahi, M., Abdollahpour, I., Abegaz, K. H., Abolhassani, H., Aboyans, V., Abreu, L. G., Abrigo, M. R. M., Abualhasan, A., Abu-Raddad, L. J., Abushouk, A. I., Adabi, M., … Lim, S. S. (2020). Global burden of 87 risk factors in 204 countries and territories, 1990–2019: A systematic analysis for the Global Burden of Disease Study 2019. *The Lancet*, *396*(10258), 1223–1249. https://doi.org/10.1016/S0140-6736(20)30752-2

Muzio, L., Viotti, A., & Martino, G. (2021). Microglia in Neuroinflammation and Neurodegeneration: From Understanding to Therapy. *Frontiers in Neuroscience*, *15*. https://www.frontiersin.org/article/10.3389/fnins.2021.742065

Myers, S., & Frumkin, H. (Eds.). (2020). *Planetary Health: Protecting Nature to Protect Ourselves*. Island Press. http://doi.org/10.5822/978-1-61091-966-1

Nakamura, S., Kugiyama, K., Sugiyama, S., Miyamoto, S., Koide, S., Fukushima, H., Honda, O., Yoshimura, M., & Ogawa, H. (2002). Polymorphism in the 5′-Flanking Region of Human Glutamate-Cysteine Ligase Modifier Subunit Gene Is Associated With Myocardial Infarction. *Circulation*, *105*(25), 2968–2973. https://doi.org/10.1161/01.CIR.0000019739.66514.1E

Nephew, B. C., Nemeth, A., Hudda, N., Beamer, G., Mann, P., Petitto, J., Cali, R., Febo, M., Kulkarni, P., Poirier, G., King, J., Durant, J. L., & Brugge, D. (2020). Traffic-related particulate matter affects behavior, inflammation, and neural integrity in a developmental rodent model. *Environmental Research*, *183*, 109242. https://doi.org/10.1016/j.envres.2020.109242

Oberdörster, G., Sharp, Z., Atudorei, V., Elder, A., Gelein, R., Kreyling, W., & Cox, C. (2004). Translocation of Inhaled Ultrafine Particles to the Brain. *Inhalation Toxicology*, *16*(6–7), 437–445. https://doi.org/10.1080/08958370490439597

Patterson, P. H. (2011). Maternal infection and immune involvement in autism. *Trends in Molecular Medicine*, *17*(7), 389–394. https://doi.org/10.1016/j.molmed.2011.03.001

Pey, J., Querol, X., Alastuey, A., Rodríguez, S., Putaud, J. P., & Van Dingenen, R. (2009). Source apportionment of urban fine and ultra-fine particle number concentration in a Western Mediterranean city. *Atmospheric Environment*, *43*(29), 4407–4415. https://doi.org/10.1016/j.atmosenv.2009.05.024

Power, M. C., Adar, S. D., Yanosky, J. D., & Weuve, J. (2016). Exposure to air pollution as a potential contributor to cognitive function, cognitive decline, brain imaging, and dementia: A systematic review of epidemiologic research. *NeuroToxicology*, *56*, 235–253. https://doi.org/10.1016/j.neuro.2016.06.004

Raz, R., Roberts, A. L., Lyall, K., Hart, J. E., Just, A. C., Laden, F., & Weisskopf, M. G. (2015). Autism spectrum disorder and particulate matter air pollution before, during, and after pregnancy: A nested case-control analysis within the Nurses' Health Study II Cohort. *Environmental Health Perspectives*, *123*(3), 264–270. https://doi.org/10.1289/ehp.1408133

Rice, C. E., Rosanoff, M., Dawson, G., Durkin, M. S., Croen, L. A., Singer, A., & Yeargin-Allsopp, M. (2012). Evaluating Changes in the Prevalence of the Autism Spectrum Disorders (ASDs). *Public Health Reviews*, *34*(2), 1–22. https://doi.org/10.1007/BF03391685

Rice, D., & Barone, S. (2000). Critical periods of vulnerability for the developing nervous system: Evidence from humans and animal models. *Environmental Health Perspectives*, *108*(Suppl 3), 511–533. https://doi.org/10.1289/ehp.00108s3511

Roberts, A. L., Lyall, K., Hart, J. E., Laden, F., Just, A. C., Bobb, J. F., Koenen, K. C., Ascherio, A., & Weisskopf, M. G. (2013). Perinatal Air Pollutant Exposures and Autism Spectrum Disorder in the Children of Nurses' Health Study II Participants. *Environmental Health Perspectives*, *121*(8), 978–984. https://doi.org/10.1289/ehp.1206187

Roqué, P. J., Dao, K., & Costa, L. G. (2016). Microglia mediate diesel exhaust particle-induced cerebellar neuronal toxicity through neuroinflammatory mechanisms. *NeuroToxicology*, *56*, 204–214. https://doi.org/10.1016/j.neuro.2016.08.006

Rutter, M. (2005). Incidence of autism spectrum disorders: Changes over time and their meaning*. *Acta Paediatrica*, *94*(1), 2–15. https://doi.org/10.1111/j.1651-2227.2005.tb01779.x

Sakurai, K., & Osumi, N. (2008). The Neurogenesis-Controlling Factor, Pax6, Inhibits Proliferation and Promotes Maturation in Murine Astrocytes. *The Journal of Neuroscience*, *28*(18), 4604–4612. https://doi.org/10.1523/JNEUROSCI.5074-07.2008

Salvi, A., & Salim, S. (2019). Neurobehavioral Consequences of Traffic-Related Air Pollution. *Frontiers in Neuroscience*, *13*. https://www.frontiersin.org/article/10.3389/fnins.2019.01232

Sandin, S., Lichtenstein, P., Kuja-Halkola, R., Larsson, H., Hultman, C. M., & Reichenberg, A. (2014). The familial risk of autism. *JAMA*, *311*(17), 1770–1777. https://doi.org/10.1001/jama.2014.4144

Schraufnagel, D. E., Balmes, J. R., Cowl, C. T., De Matteis, S., Jung, S.-H., Mortimer, K., Perez-Padilla, R., Rice, M. B., Riojas-Rodriguez, H., Sood, A., Thurston, G. D., To, T., Vanker, A., & Wuebbles, D. J. (2019). Air Pollution and Noncommunicable Diseases: A Review by the Forum of International Respiratory Societies' Environmental Committee, Part 2: Air Pollution and Organ Systems. *Chest*, *155*(2), 417–426. https://doi.org/10.1016/j.chest.2018.10.041

Shi, L., Wu, X., Yazdi, M. D., Braun, D., Awad, Y. A., Wei, Y., Liu, P., Di, Q., Wang, Y., Schwartz, J., Dominici, F., Kioumourtzoglou, M.-A., & Zanobetti, A. (2020). Long-term effects of PM2·5 on neurological disorders in the American Medicare population: A longitudinal cohort study. *The Lancet Planetary Health*, *4*(12), e557–e565. https://doi.org/10.1016/S2542-5196(20)30227-8

Spijker, S. (2011). Dissection of Rodent Brain Regions. In K. W. Li (Ed.), *Neuroproteomics* (Vol. 57, pp. 13–26). Humana Press. https://doi.org/10.1007/978-1-61779-111-6_2

Suades-González, E., Gascon, M., Guxens, M., & Sunyer, J. (2015). Air Pollution and Neuropsychological Development: A Review of the Latest Evidence. *Endocrinology*, *156*(10), 3473–3482. https://doi.org/10.1210/en.2015-1403

Suglia, S. F., Gryparis, A., Wright, R. O., Schwartz, J., & Wright, R. J. (2008). Association of Black Carbon with Cognition among Children in a Prospective Birth Cohort Study. *American Journal of Epidemiology*, *167*(3), 280–286. https://doi.org/10.1093/aje/kwm308

Sunyer, J., Esnaola, M., Alvarez-Pedrerol, M., Forns, J., Rivas, I., López-Vicente, M., Suades-González, E., Foraster, M., Garcia-Esteban, R., Basagaña, X., Viana, M., Cirach, M., Moreno, T., Alastuey, A., Sebastian-Galles, N., Nieuwenhuijsen, M., & Querol, X. (2015). Association between Traffic-Related Air Pollution in Schools and Cognitive Development in Primary School Children: A Prospective Cohort Study. *PLOS Medicine*, *12*(3), e1001792. https://doi.org/10.1371/journal.pmed.1001792

Suzuki, T., Oshio, S., Iwata, M., Saburi, H., Odagiri, T., Udagawa, T., Sugawara, I., Umezawa, M., & Takeda, K. (2010). In utero exposure to a low concentration of diesel exhaust affects spontaneous locomotor activity and monoaminergic system in male mice. *Particle and Fibre Toxicology*, *7*(1), 7. https://doi.org/10.1186/1743-8977-7-7

Tuoc, T. C., Radyushkin, K., Tonchev, A. B., Piñon, M. C., Ashery-Padan, R., Molnár, Z., Davidoff, M. S., & Stoykova, A. (2009). Selective Cortical Layering Abnormalities and Behavioral Deficits in Cortex-Specific Pax6 Knock-Out Mice. *Journal of Neuroscience*, *29*(26), 8335–8349. https://doi.org/10.1523/JNEUROSCI.5669-08.2009

Umeda, T., Takashima, N., Nakagawa, R., Maekawa, M., Ikegami, S., Yoshikawa, T., Kobayashi, K., Okanoya, K., Inokuchi, K., & Osumi, N. (2010). Evaluation of Pax6 Mutant Rat as a Model for Autism. *PLOS ONE*, *5*(12), e15500. https://doi.org/10.1371/journal.pone.0015500

UNECE. (n.d.). *Air pollution and health | UNECE*. Retrieved May 13, 2022, from https://unece.org/air-pollution-and-health

US EPA, O. (2020, April 13). *National Ambient Air Quality Standards (NAAQS) for PM* [Other Policies and Guidance]. https://www.epa.gov/pm-pollution/national-ambient-air-quality-standards-naaqs-pm

US EPA (United States Environemntal Protection Agency). (2002). *Health Assessment Document for Diesel Engine Exhaust* (p. 669). National Center for Environemntal Assessment, USEPA. https://cfpub.epa.gov/ncea/risk/recordisplay.cfm?deid=29060

Vedal, S., Campen, M. J., McDonald, J. D., Larson, T. V., Sampson, P. D., Sheppard, L., Simpson, C. D., & Szpiro, A. A. (2013). National Particle Component Toxicity (NPACT) initiative report on cardiovascular effects. Research report (Health Effects Institute), (178), 5–8.

Veronesi, B., Makwana, O., Pooler, M., & Chen, L. C. (2005). Effects of Subchronic Exposures to Concentrated Ambient Particles: VII. Degeneration of Dopaminergic Neurons in Apo E−/− Mice. *Inhalation Toxicology*, *17*(4–5), 235–241. https://doi.org/10.1080/08958370590912888

Volk, H. E., Hertz-Picciotto, I., Delwiche, L., Lurmann, F., & McConnell, R. (2011). Residential Proximity to Freeways and Autism in the CHARGE Study. *Environmental Health Perspectives*, *119*(6), 873–877. https://doi.org/10.1289/ehp.1002835

Volk, H. E., Kerin, T., Lurmann, F., Hertz-Picciotto, I., McConnell, R., & Campbell, D. B. (2014). Brief Report: Autism Spectrum Disorder: Interaction of Air Pollution with the MET Receptor Tyrosine Kinase Gene. *Epidemiology*, *25*(1), 44–47. http://www.jstor.org/stable/24759022

Volk, H. E., Lurmann, F., Penfold, B., Hertz-Picciotto, I., & McConnell, R. (2013). Traffic-Related Air Pollution, Particulate Matter, and Autism. *JAMA Psychiatry*, *70*(1), 71–77. https://doi.org/10.1001/jamapsychiatry.2013.266

Wang, X., Wang, Y., Bai, Y., Wang, P., & Zhao, Y. (2019). An overview of physical and chemical features of diesel exhaust particles. *Journal of the Energy Institute*, *92*(6), 1864–1888. https://doi.org/10.1016/j.joei.2018.11.006

Weitekamp, C. A., Kerr, L. B., Dishaw, L., Nichols, J., Lein, M., & Stewart, M. J. (2020). A systematic review of the health effects associated with the inhalation of particle-filtered and whole diesel exhaust. *Inhalation Toxicology*, *32*(1), 1–13. https://doi.org/10.1080/08958378.2020.1725187

Weldy, C. S., White, C. C., Wilkerson, H.-W., Larson, T. V., Stewart, J. A., Gill, S. E., Parks, W. C., & Kavanagh, T. J. (2011). Heterozygosity in the glutathione synthesis gene Gclm increases sensitivity to diesel exhaust particulate induced lung inflammation in mice. *Inhalation Toxicology*, *23*(12), 724–735. https://doi.org/10.3109/08958378.2011.608095

Wu, W., Jin, Y., & Carlsten, C. (2018). Inflammatory health effects of indoor and outdoor particulate matter. *Journal of Allergy and Clinical Immunology*, *141*(3), 833–844. https://doi.org/10.1016/j.jaci.2017.12.981

Wu, X., Zhao, W., Cui, Q., & Zhou, Y. (2020). Computational screening of potential regulators for mRNA-protein expression level discrepancy. *Biochemical and Biophysical Research Communications*, *523*(1), 196–201. https://doi.org/10.1016/j.bbrc.2019.12.052

Xu, X., Ha, S. U., & Basnet, R. (2016). A Review of Epidemiological Research on Adverse Neurological Effects of Exposure to Ambient Air Pollution. *Frontiers in Public Health*, *4*. https://www.frontiersin.org/article/10.3389/fpubh.2016.00157

Yale Center for Environmental Law and Policy. (n.d.). *Welcome | Environmental Performance Index*. Retrieved June 3, 2021, from https://epi.yale.edu/

Ye, Y. (2016, January 6). Autism in Mice: Developing Behavioral Standards. *Maze Engineers*. https://conductscience.com/maze/autism-in-mice-models/

Yin, F., Lawal, A., Ricks, J., Fox, J. R., Larson, T., Navab, M., Fogelman, A. M., Rosenfeld, M. E., & Araujo, J. A. (2013, June). *Diesel Exhaust Induces Systemic Lipid Peroxidation and Development of Dysfunctional Pro-Oxidant and Pro-Inflammatory High-Density Lipoprotein*. https://doi.org/10.1161/ATVBAHA.112.300552

Yoshizaki, K., Furuse, T., Kimura, R., Tucci, V., Kaneda, H., Wakana, S., & Osumi, N. (2016). Paternal Aging Affects Behavior in Pax6 Mutant Mice: A Gene/Environment Interaction in Understanding Neurodevelopmental Disorders. *PLOS ONE*, *11*(11), e0166665. https://doi.org/10.1371/journal.pone.0166665

Zeidan, J., Fombonne, E., Scorah, J., Ibrahim, A., Durkin, M. S., Saxena, S., Yusuf, A., Shih, A., & Elsabbagh, M. (2022). Global prevalence of autism: A systematic review update. *Autism Research*, *15*(5), 778–790. https://doi.org/10.1002/aur.2696

Zhang, H., & Forman, H. J. (2009). Signaling pathways involved in phase II gene induction by α, β-unsaturated aldehydes. *Toxicology and Industrial Health*, *25*(4–5), 269–278. https://doi.org/10.1177/0748233709102209

Zikopoulos, B., & Barbas, H. (2010). Changes in prefrontal axons may disrupt the network in autism. *The Journal of Neuroscience: The Official Journal of the Society for Neuroscience*, *30*(44), 14595–14609. https://doi.org/10.1523/JNEUROSCI.2257-10.2010

Appendix

Primer Sequences

- *Cd68:* F (5’ ACTGGTGTAGCCTAGCTGGT 3’)
  R (5’ CCTTGGGCTATAAGCGGTCC3’)
- *Gapdh:* F (5’ TGACCTCAACTACATGGTCTACA 3’)
  R (5’ CTTCCCATTCTCGGCCTTG 3’)
- *Iba1:* F (5’ CTTGAAGCGAATGCTGGAGAA 3’)
  R (5’ GGCAGCTCGGAGATAGCTTT 3’)
- *Ifnγ:* F (5’ TCAAGTGGCATAGATGTGGAAGAA 3’)
  R (5’ TGGCTCTGCAGGATTTTCATG 3’)
- *Il-1β:* F (5’ CAACCAACAAGTGATATTCTCCATG 3’)
  R (5’ ATCCACACTCTCCAGCTGCA 3’)
- *Il-4:* F (5’ ACAGGAGAAGGGACGCCAT 3’)
  R (5’ GAAGCCCTACAGACGAGCTCA 3’)
- *Il-6:* F (5’ GAGGATACCACTCCCAACAGACC 3’)
  R (5’ AAGTGCATCATCGTTGTTCATACA 3’)
- *Pax6:* F (5’ ACTTTAACCAAGGGCGGTGAG 3’)
  R (5’ TTCACTCCGCTGTGACTGTTC 3’)
- *Stat1:* F (5’ TCCCGTACAGATGTCCATGAT 3’)
  R (5’ CTGAATATTTCCCTCCTGGG 3’)
- *Stat6:* F (5’ GAGTTCCTGGTCGGTTCAGA 3’)
  R (5’ GCTCTCCAAGGTGCTGATGT 3’)
- *Tnfα:* F (5’ GCCTCTTCTCATTCCTGCTTG 3’)
  R (5’ CTGATGAGAGGGAGGCCATT 3’)